23rd Asia-Pacific Regional Space Agency Forum

Sofitel Hotel, Manila, Philippines
November 15-18, 2016

Space Weather and Seismoelectromagnetics in the Philippines

R. E. S. Otadoy, R. Violanda, and P. Ong
Theoretical and Computational Sciences and Engineering (TCSE) Group, Department of Physics, University of San Carlos, Cebu City, Philippines
Center for Geoinformatics and Environmental Solutions, University of San Carlos, Cebu City, Philippines

I. Yoshikawa, T. Uozumi, S. Abe, and A. Fujimoto
International Center for Space Weather Science and Education (ICSWSE), Kyushu University, Fukuoka, Japan

H. Ishibashi and T. Nagatsuma
National Institute of Information and Communications Technology (NICT), Tokyo, Japan

Q. Sugon Jr. and D. McNamara
ICSWSE Subcenter, Manila Observatory, Quezon City, Philippines

From SERC to ICSWSE…

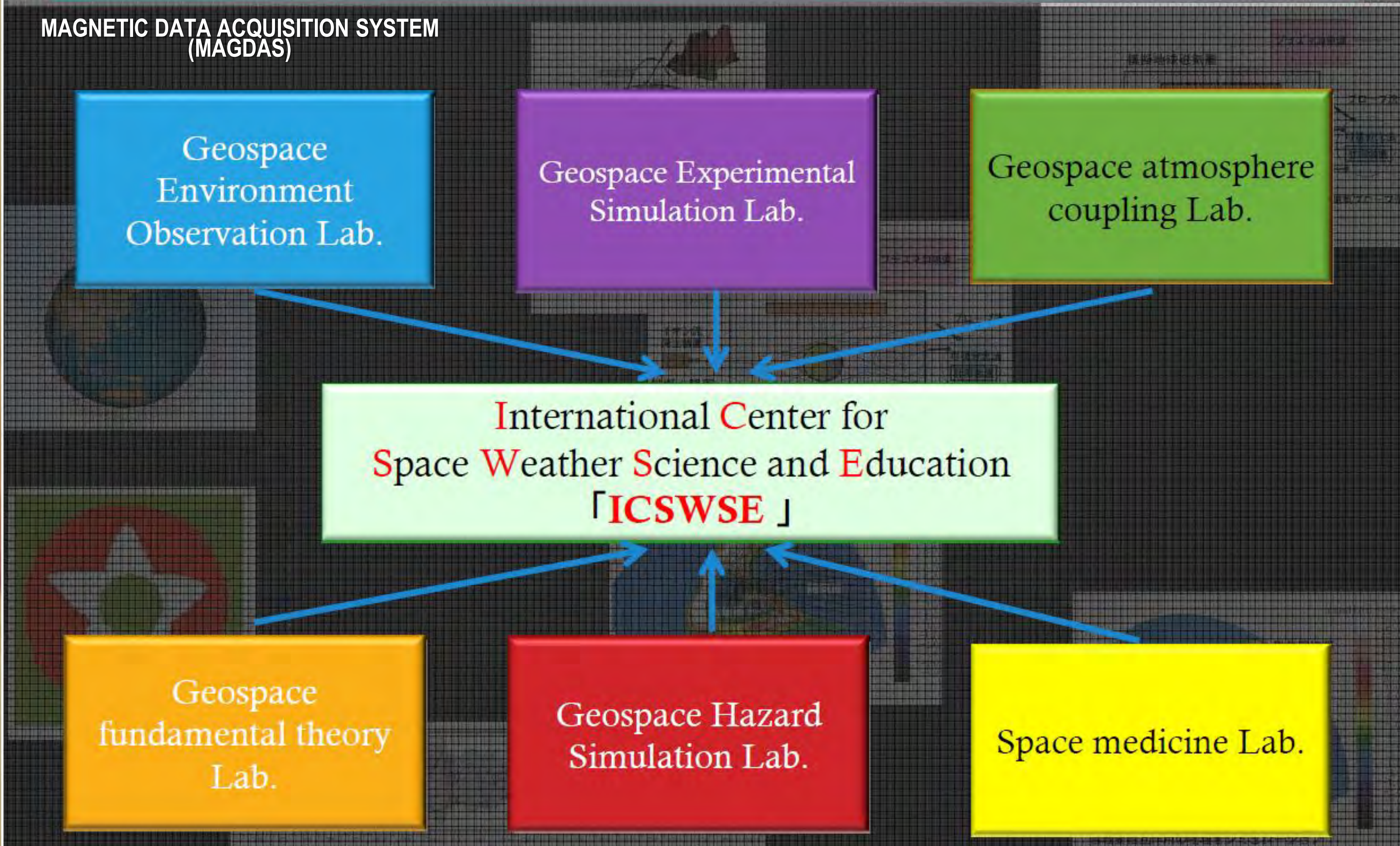

MAGNETIC DATA ACQUISITION SYSTEM (MAGDAS)

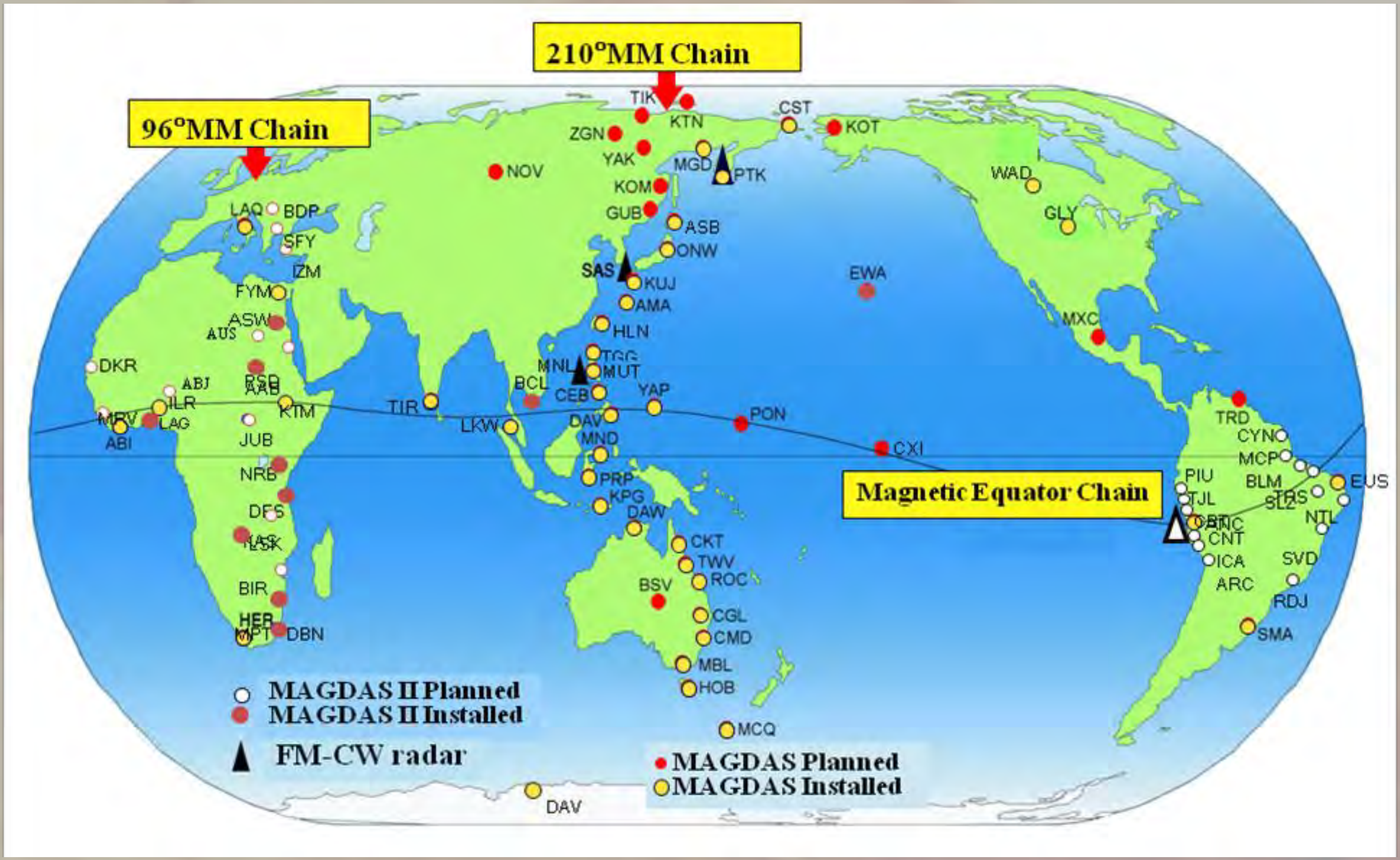

Space environment monitoring: Geomagnetic field disturbances

MAGDAS/CPMN started in 2003
(MAGnetic Data Acquisition System/Circum pan Pacific Magnetometer Array)

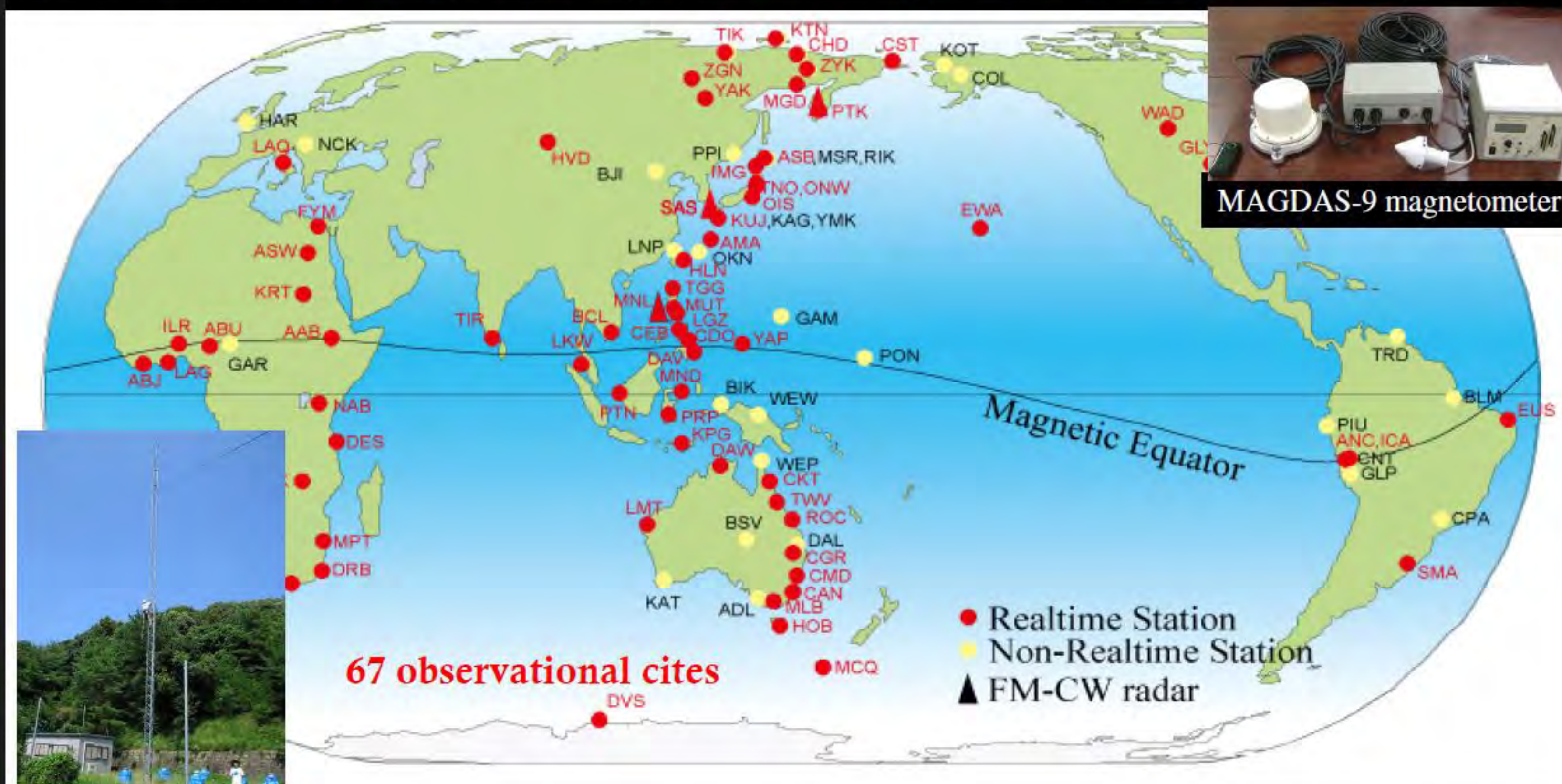

MAGDAS-9 magnetometer

About NICT

- The "ONLY National Institute" of Information and Communications technology in Japan
- Staff: permanent researchers: 300, temporal researchers: 400, administrative: 200 (approximately).
- Yearly budget: about 30 billion JPY
- Headquarter: Koganei, Tokyo
- Main Blanches: Keihanna, Kobe, Kashima, Okinawa
- Domestic Space Weather Observatories: Wakkanai, Hiraiso, Yamagawa, Okinawa

NICT ionospheric observation network

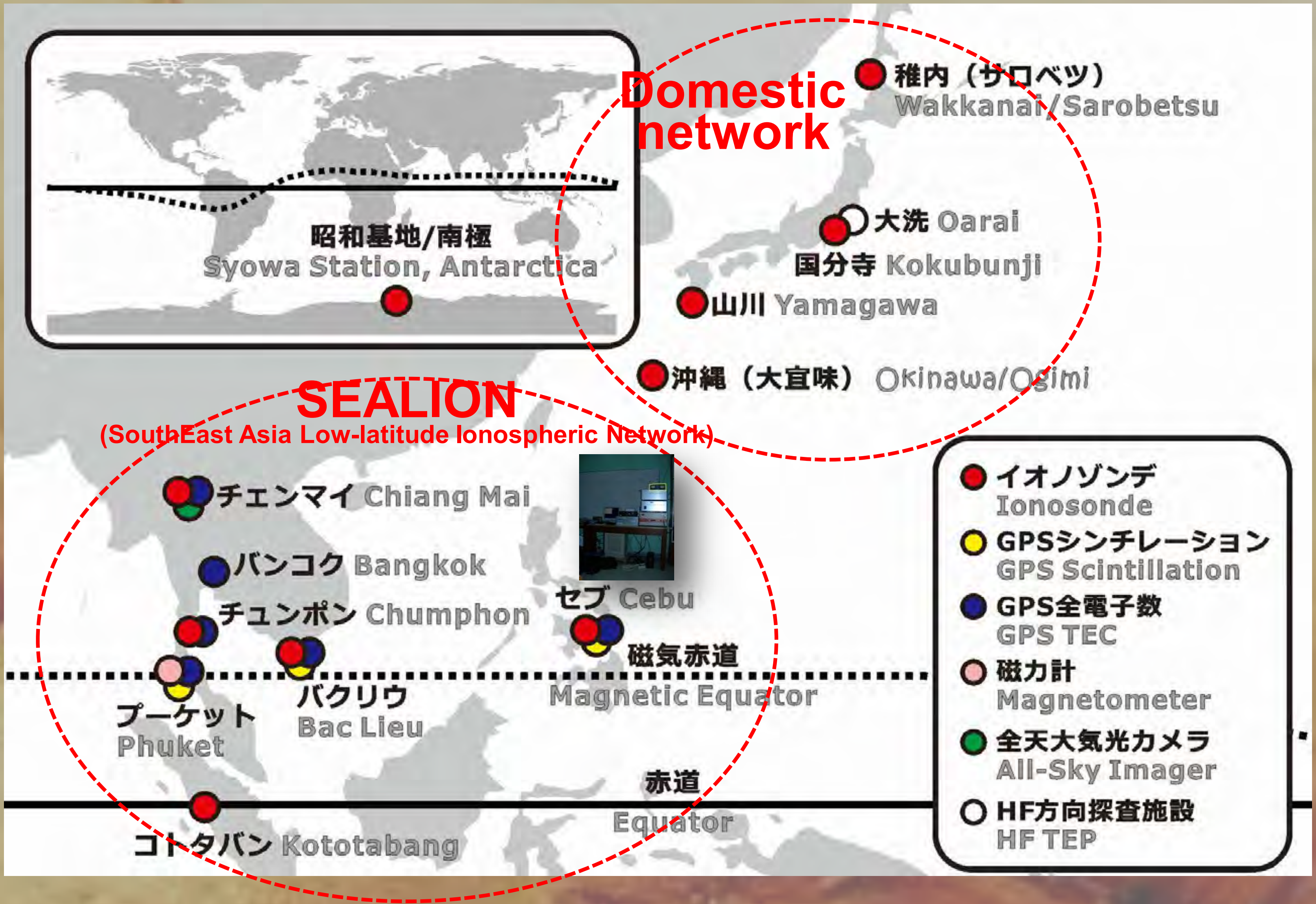

Two parts of presentation:

- Space weather (equatorial electrojet)
- Seismoelectromagnetics

- The source of all energy (nuclear fusion) in the solar system
- mostly composed of hydrogen
- radius is about 700,000 km, 110 times the radius of the earth
- mass is $2X10^{30}$ kg about $3.3X10^{5}$ times the mass of earth

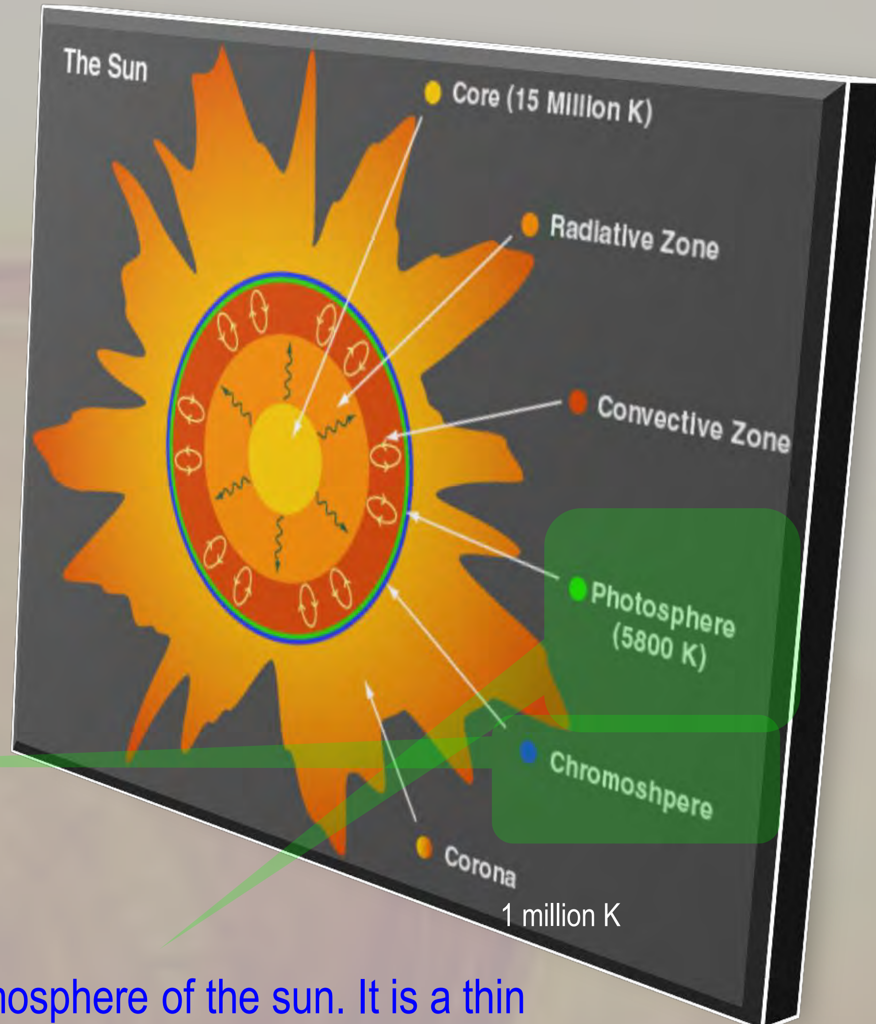

About 2000km thick, temperature is 10^{5} K

Defines the atmosphere of the sun. It is a thin layer, about 500km.

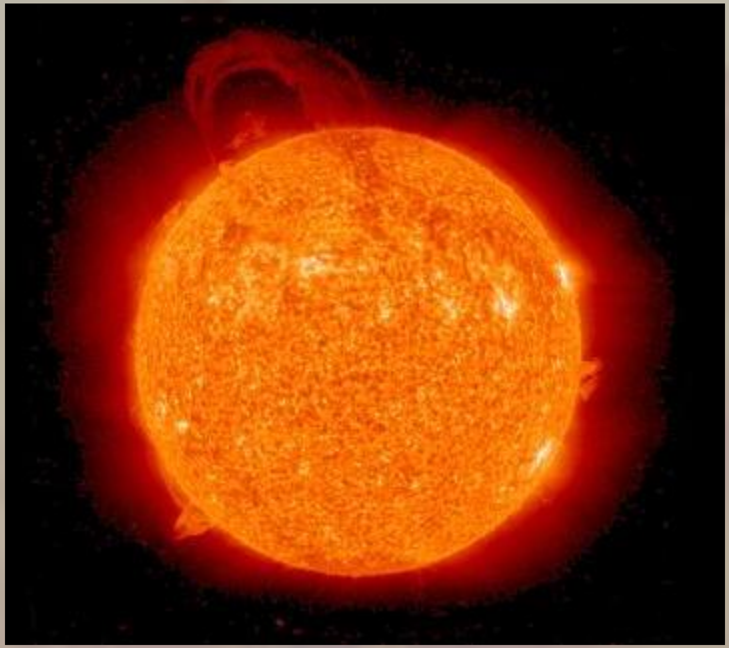

Prominence April 12-13, 2010.

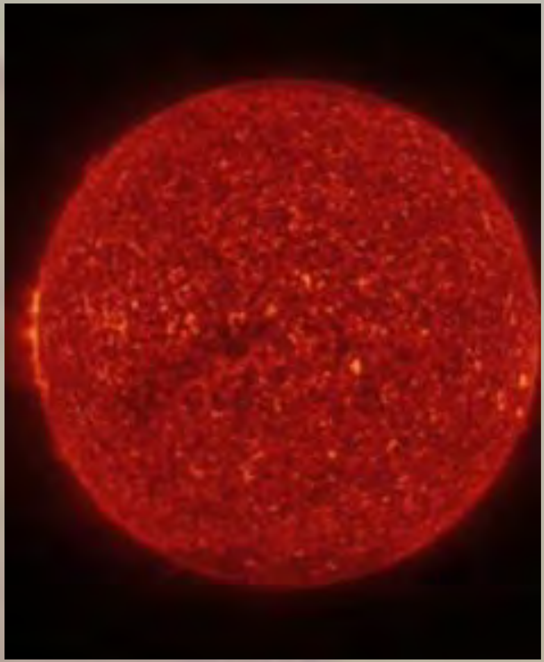

March 17-27, 2007

Image above: STEREO's (Solar Terrestrial Relations Observatory) Extreme Ultraviolet Imaging Telescope captured these images of the sun
Courtesy: **NASA**

THE EARTH'S ATMOSPHERE AND IONOSPHERE

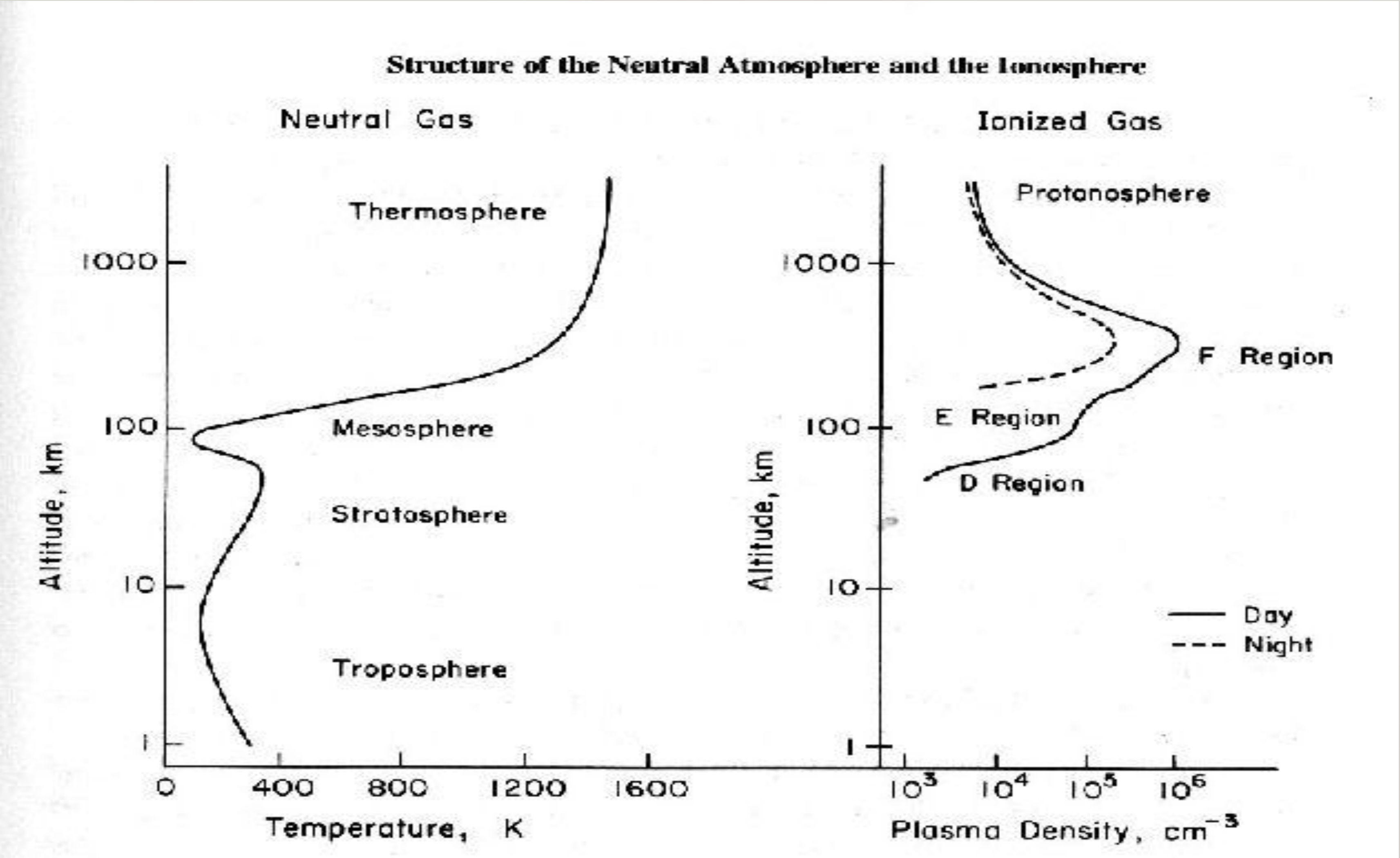

THE EARTH'S MAGNETIC FIELD

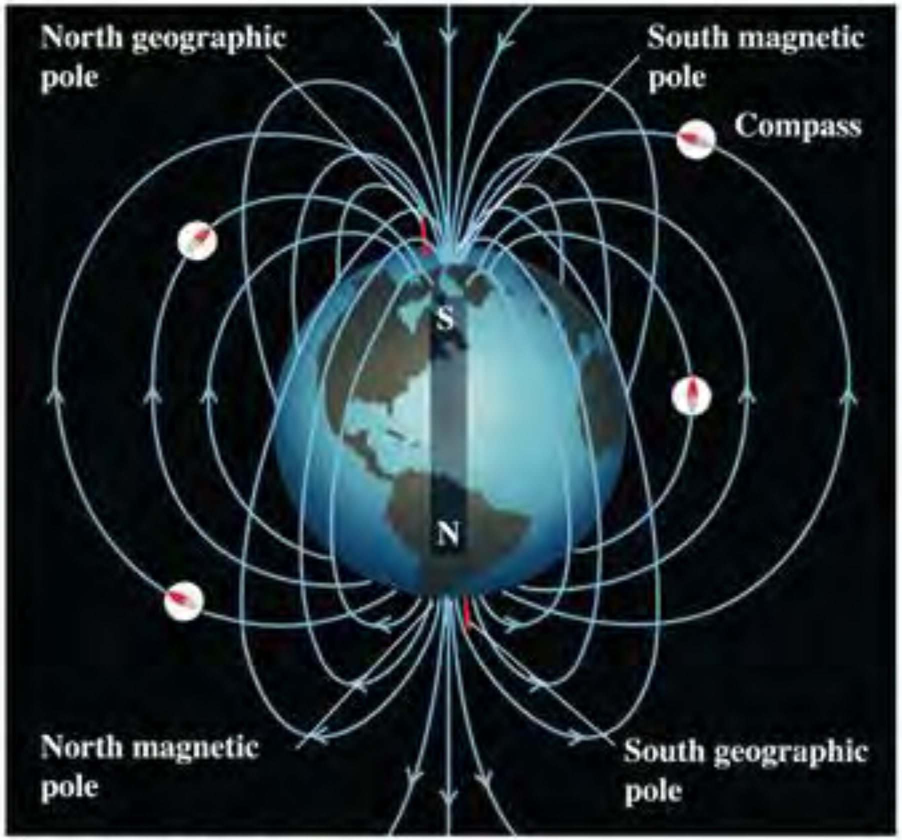

THE SOLAR WIND

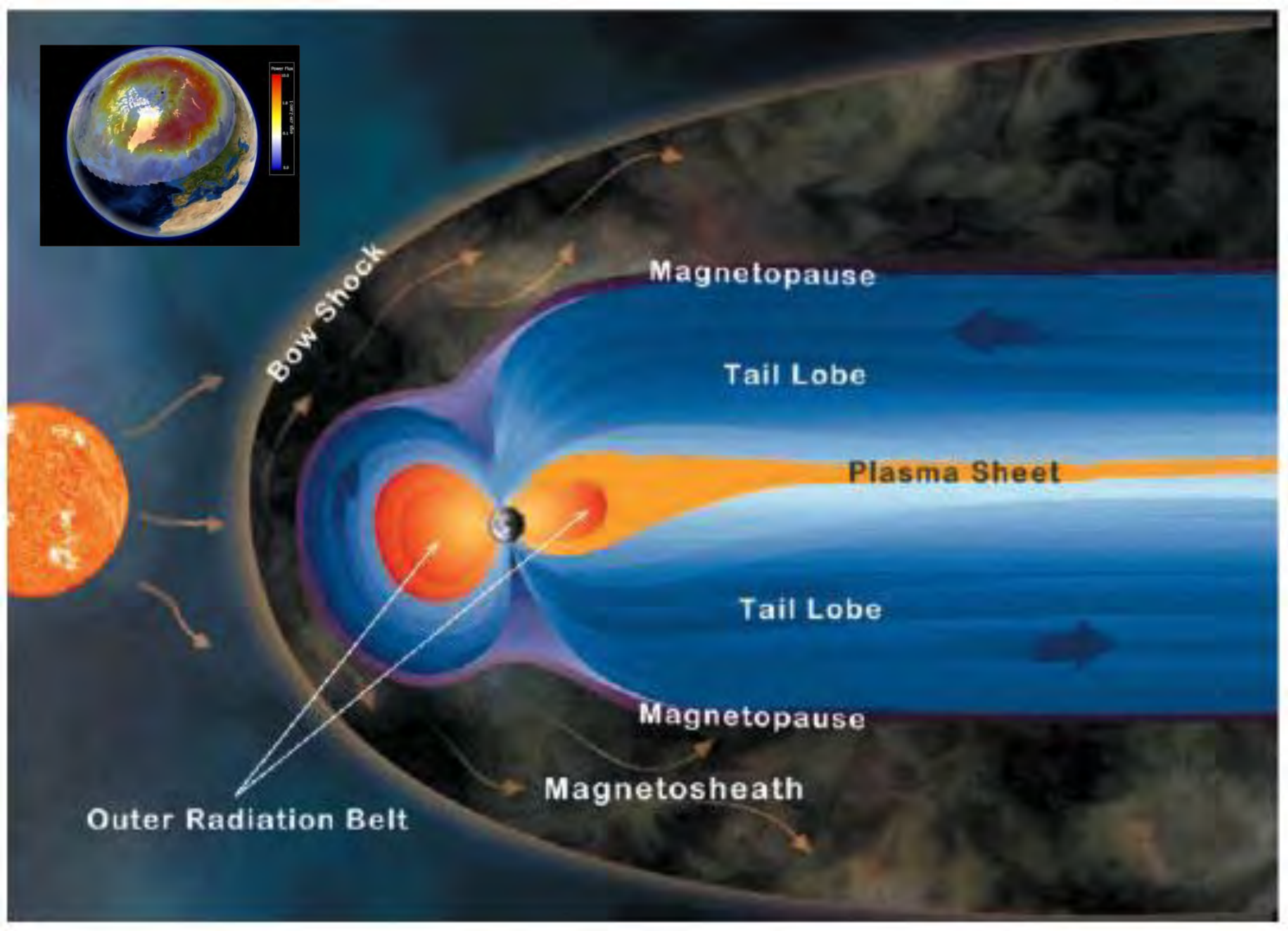

Lyon, J. G., The solar wind-magnetosphere-ionosphere-coupling, *Science*, **288**(5473), 1987-1991, 2000.

SPACE STORM

First detected by Alexander von Humboldt

2003,10/28 Event
10UT 〜X17.2

10/29 Event
21UT〜X10.0

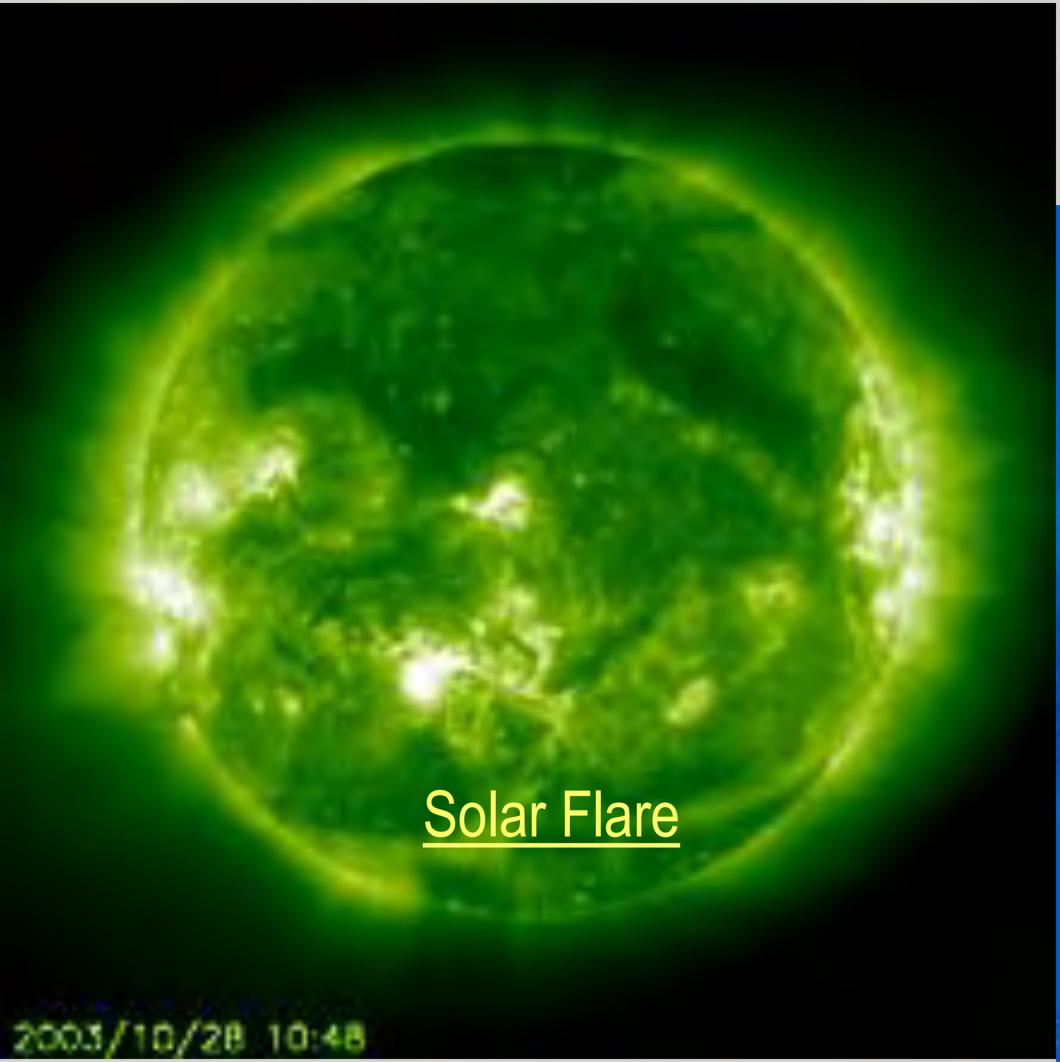

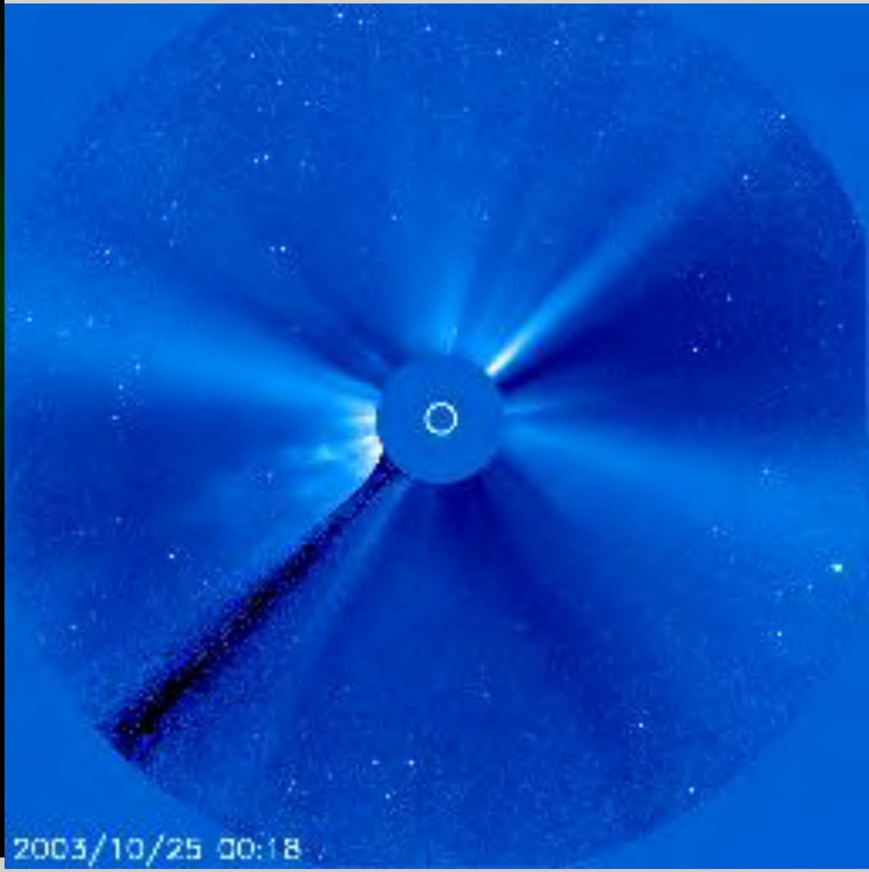

Coronal Mass Ejection

Harmful effects of space storms:

- geomagnetically induced currents can damage power stations (Brazil and Canada)

(Boteler, D.H., R.M. Shier, T. Watanabe and R.E. Horita, Effects of geomagneticlly induced currents in the B.C. Hydro 500 kV system, *IEEE Trans. Power Delivery*, **4**, 818-823, 1989.)

- Increase drag of satellitess
- Disrupt satellite communications
- Highly energetic charged particles may be harmful

MAGDAS Magnetometer Array

EQUATORIAL ELECTROJET

- The equatorial electrojet or EEJ (Chapman 1951) is a narrow band of current at the E-region of the ionosphere flowing eastward along the dayside dip equator.

- It is caused by the enhancement of east-west Pedersen conductivity and manifests as an enhancement of the daily variations of the northward component *H* of the geomagnetic field with the maximum occurring at the dip equatorial latitudes.

- It was first detected at Huancayo, Peru in 1922.

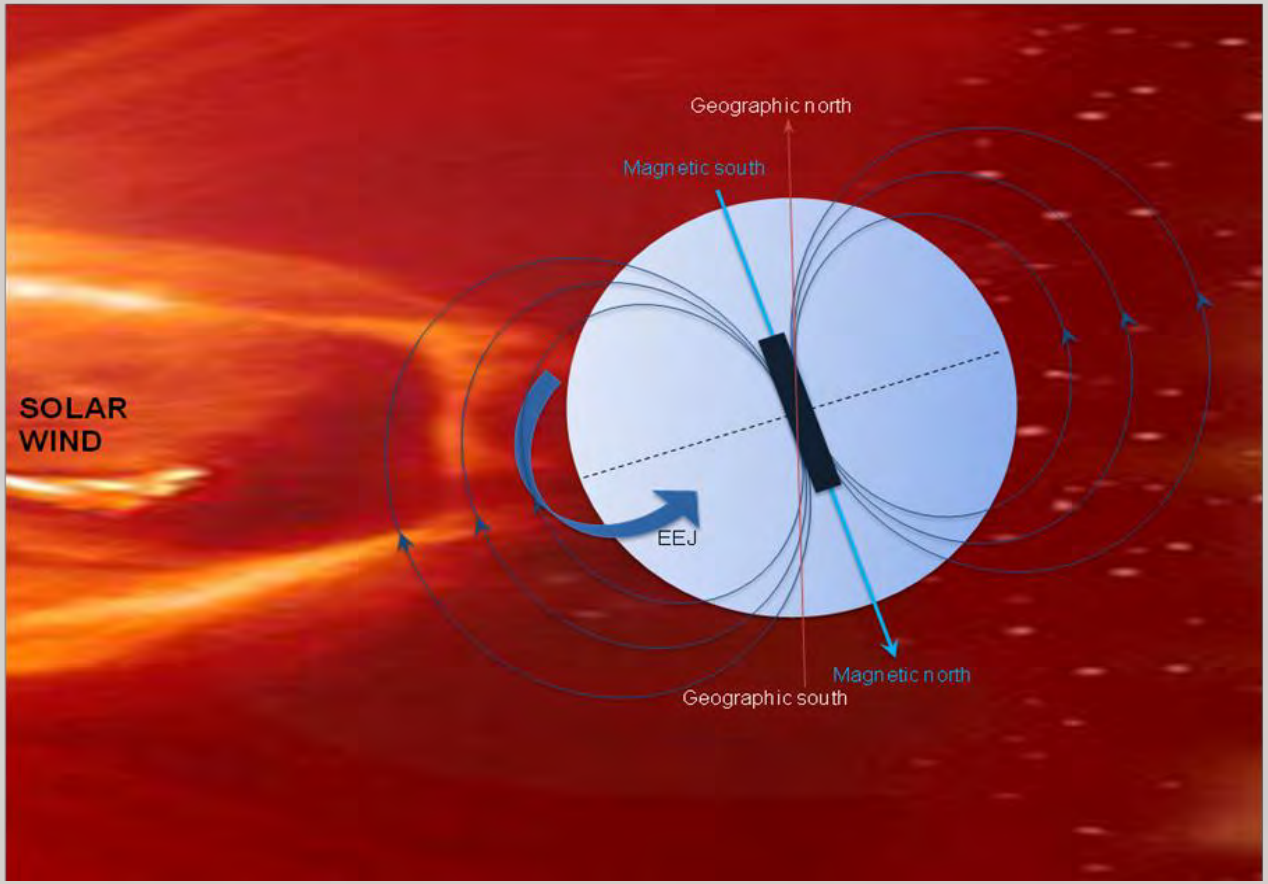

Ueno et al.(2008)

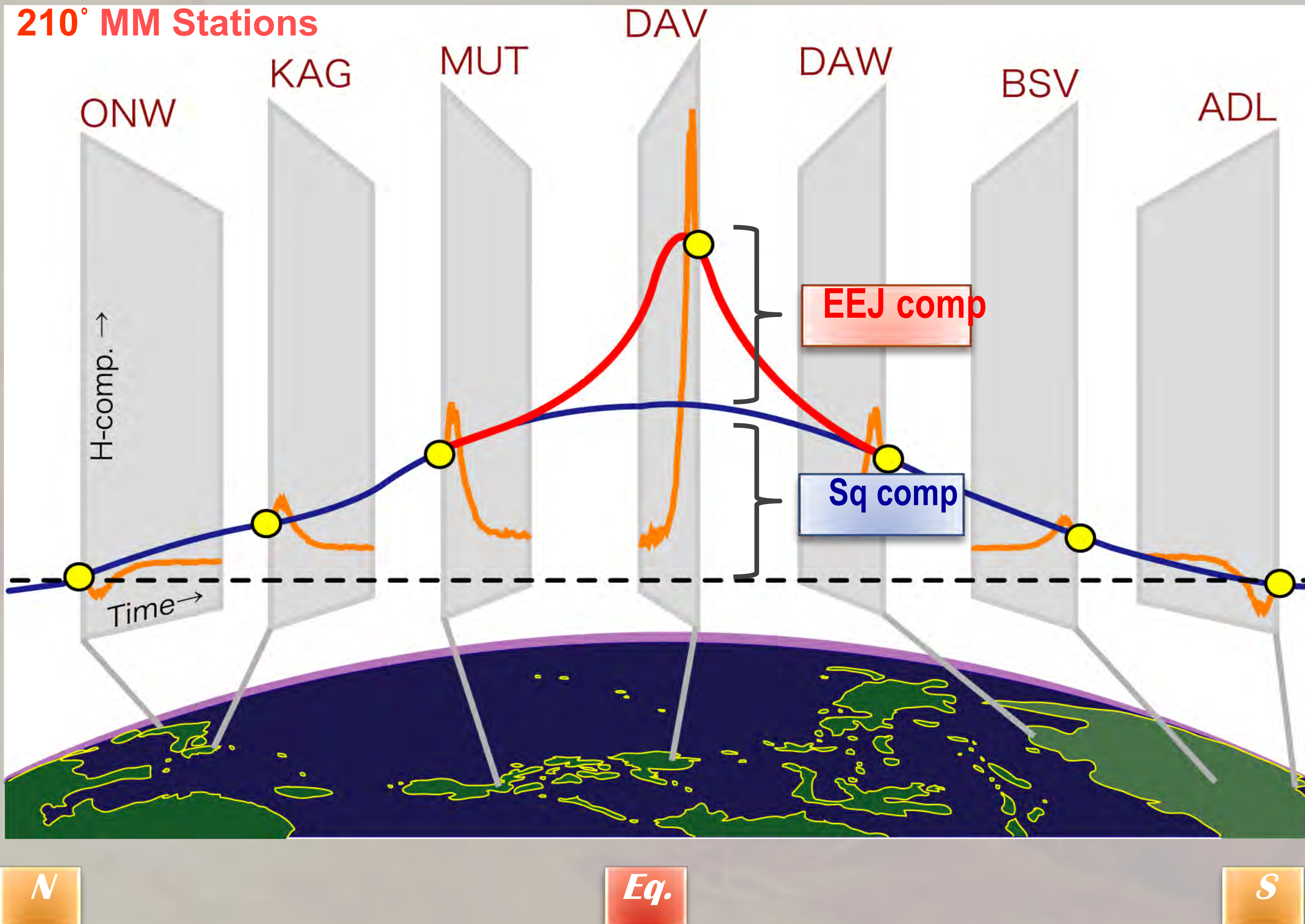

2001/09/01

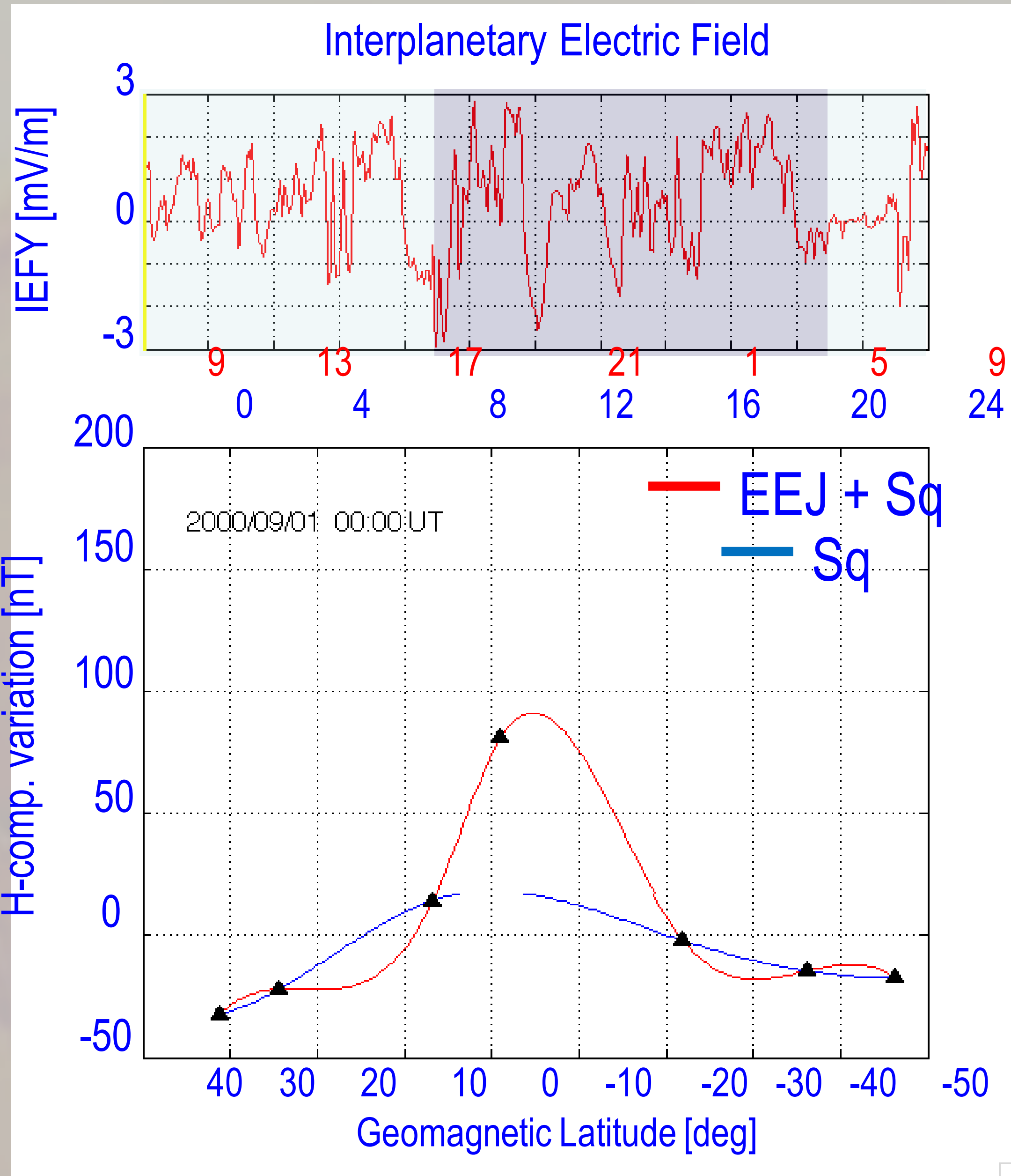

Ueno et al.(2008)

EE-Index (*EDst, EU, EL*)

Uozumi et al. (2009)

Definition of *EDst*

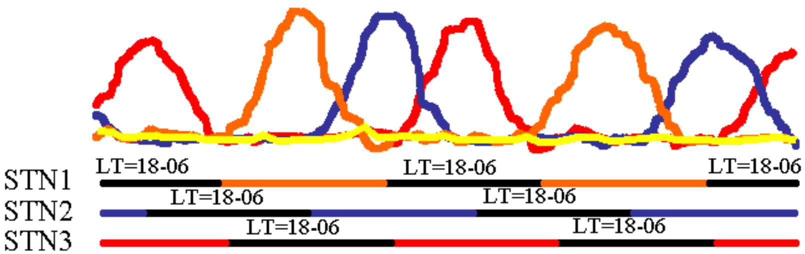

$$EDst(m) = \sum_{S|_{LT=18\text{-}06}} ER_S(m)\Big|_{LT=18\text{-}06} \Big/ N(m)\Big|_{LT=18\text{-}06}$$

S: index of station

m: point of time in UT

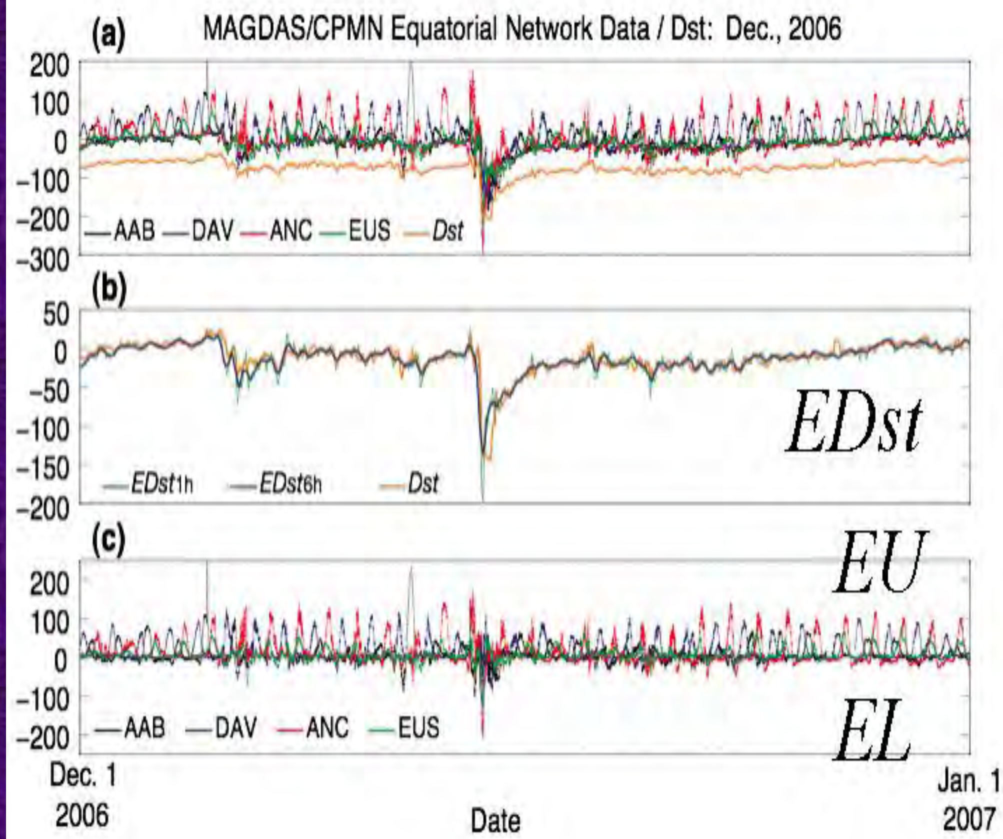

EDst : the mean value of magnetic fields at night side.

EU: Amplitude of EEJ

EL: Amplitude of CEJ

A new *EE*-index to monitor short- and long-term variations of the equatorial electrojet by adopting the MAGDAS/CPMN real-time data.

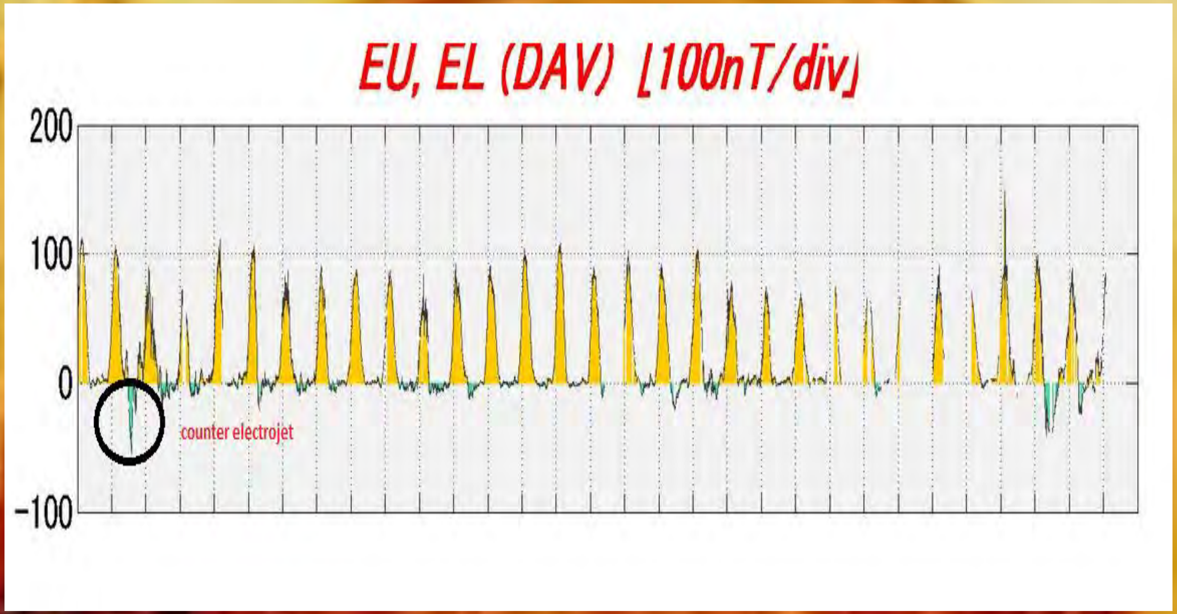
EU, EL (DAV) [100nT/div]
200
100
0
-100
counter electrojet

Seismoelectromagnetics

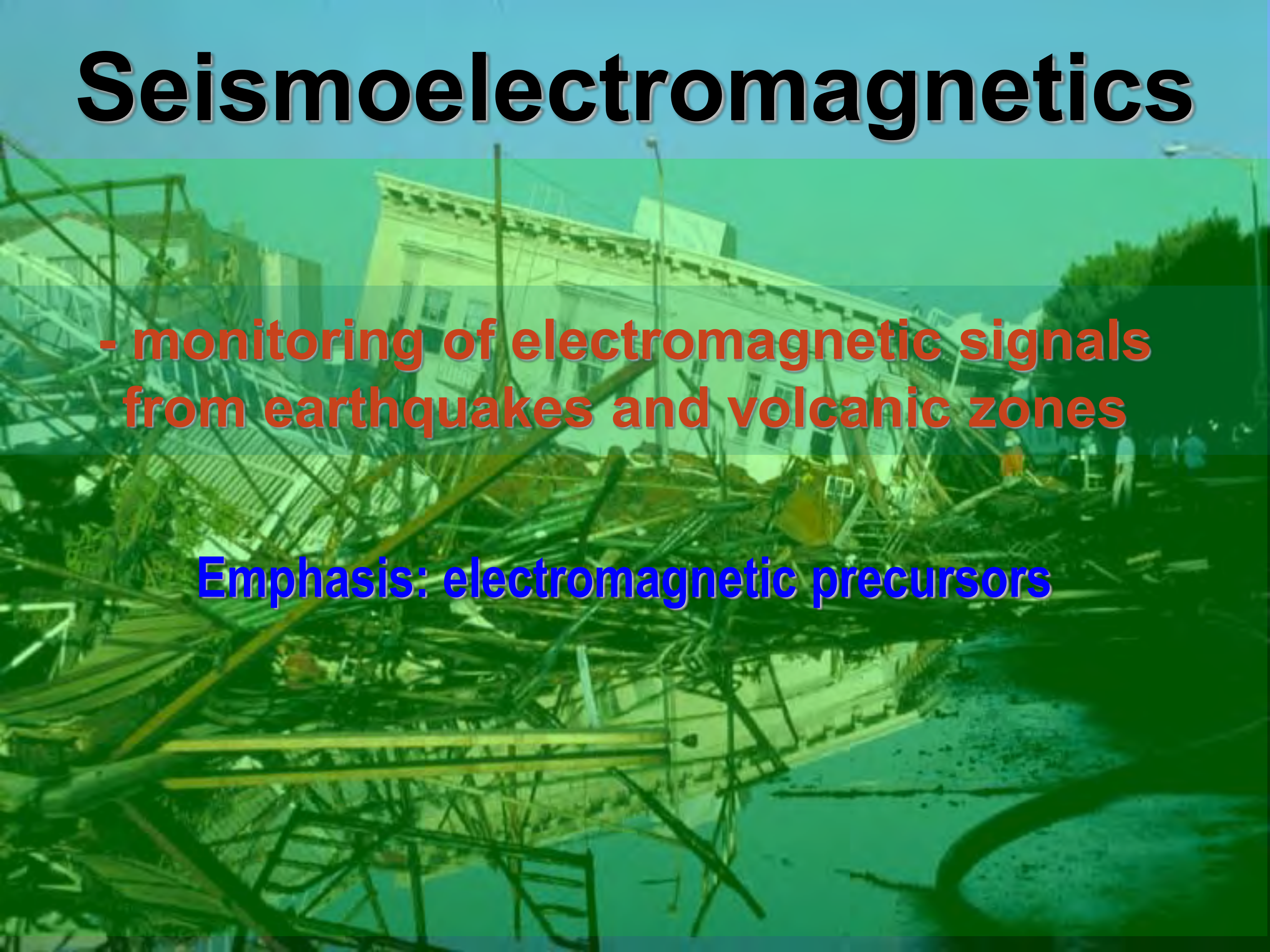

- monitoring of electromagnetic signals from earthquakes and volcanic zones

Emphasis: electromagnetic precursors

Outline

1. Sample observations of EM earthquake precursors
2. Mechanisms
3. What we can do through our collaborations
4. Conclusion

Sample Observations of Electromagnetic (wideband of frequencies from ULF to optical) Signatures of Earthquake

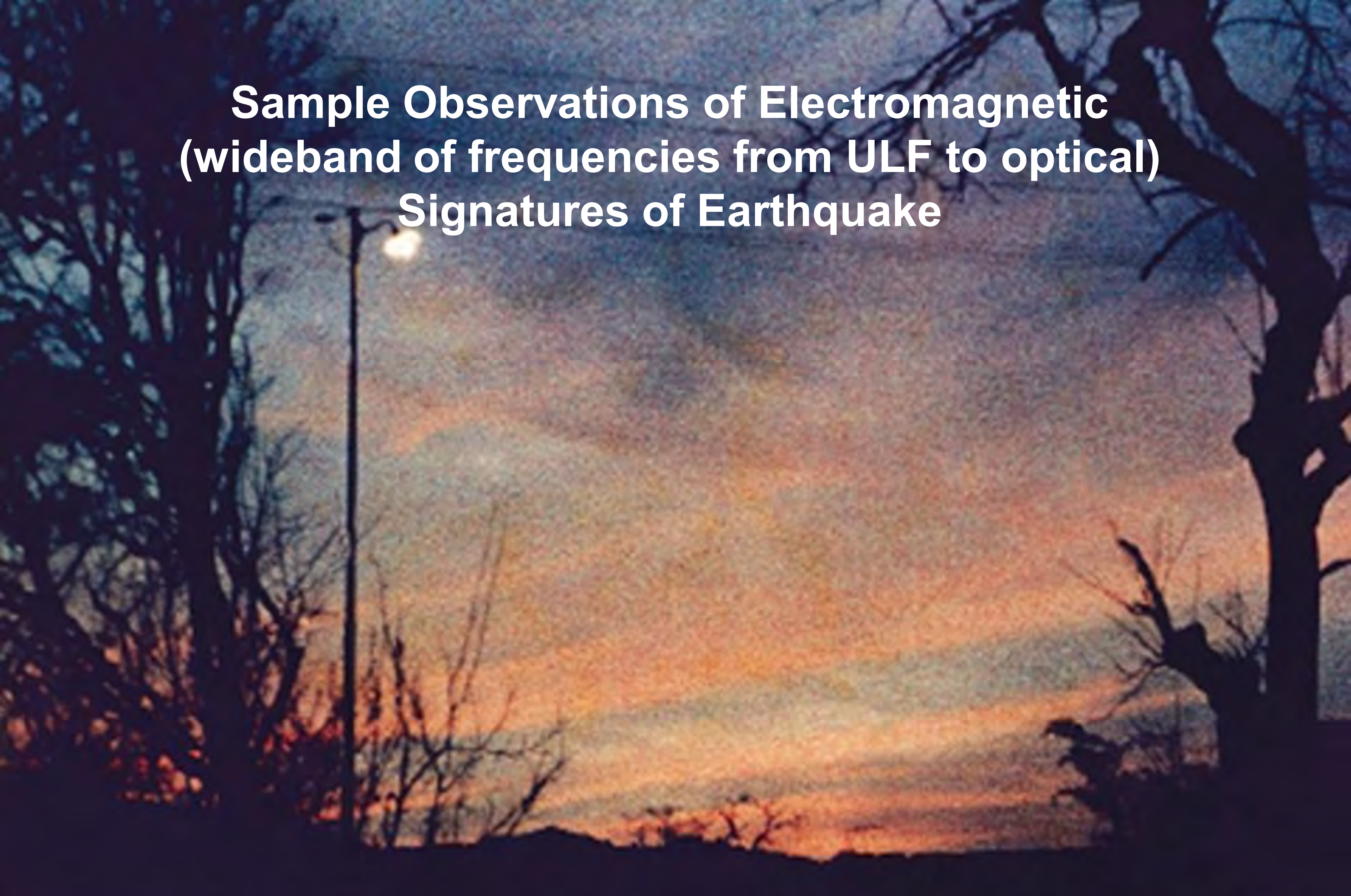

MYSTERIOUS LIGHTS: Changes in the ion concentration in the air could be the cause of lights such as these, seen prior to a Japanese earthquake in 1966.

- **Optical – Kobe 1995, white, blue, orange extending 200 m up in the air and 1 to 8 km across the ground.**

- **ULF radio band (ultra low frequency; 1 to 10 Hertz) – 1989 Loma Prieta earthquake; 2 weeks the ULF signal was 20 times of the normal background noise; 3 hours before it climbed 60 times**

- **ELF – 2003 San Simeon, California**

- **Infrared – 2001 Gujarat, India**

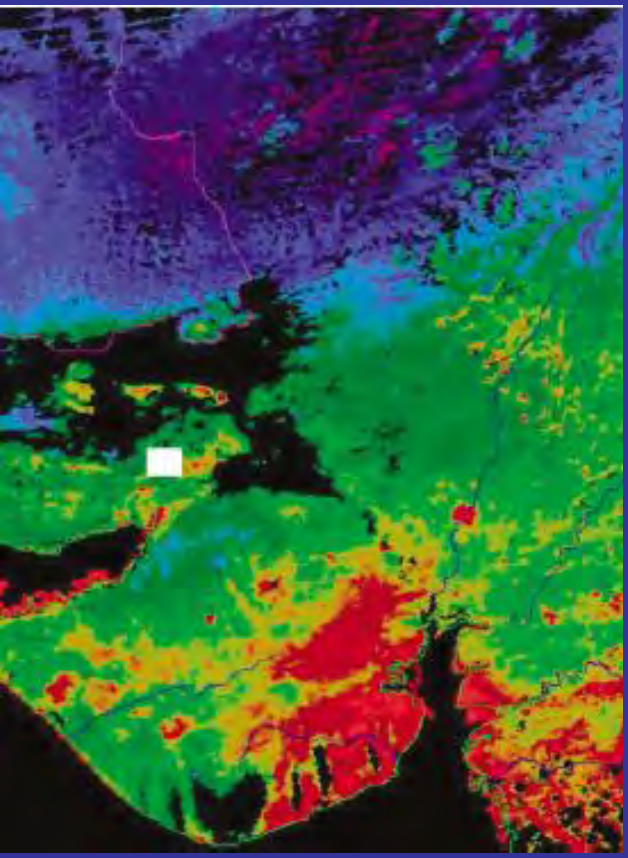

January 6, 2001

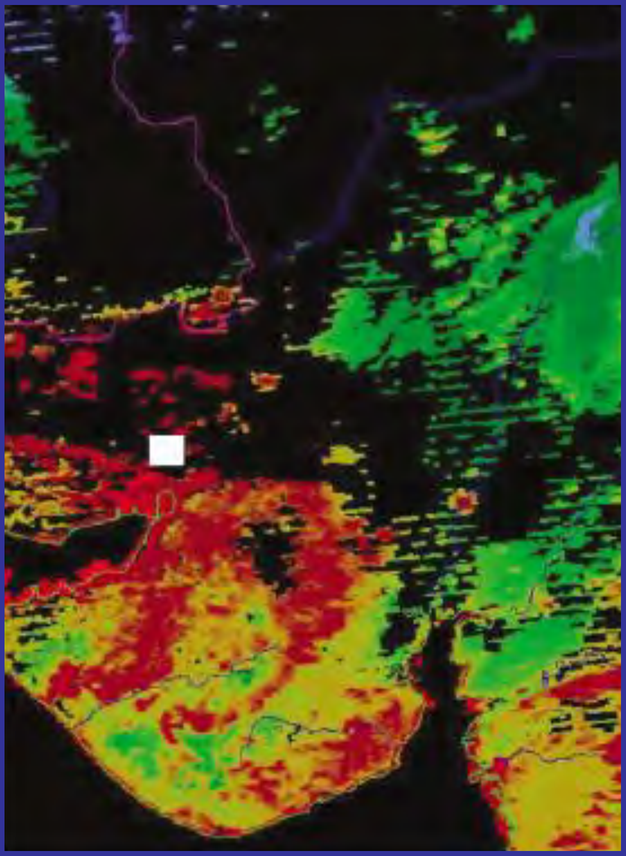

January 21, 2001

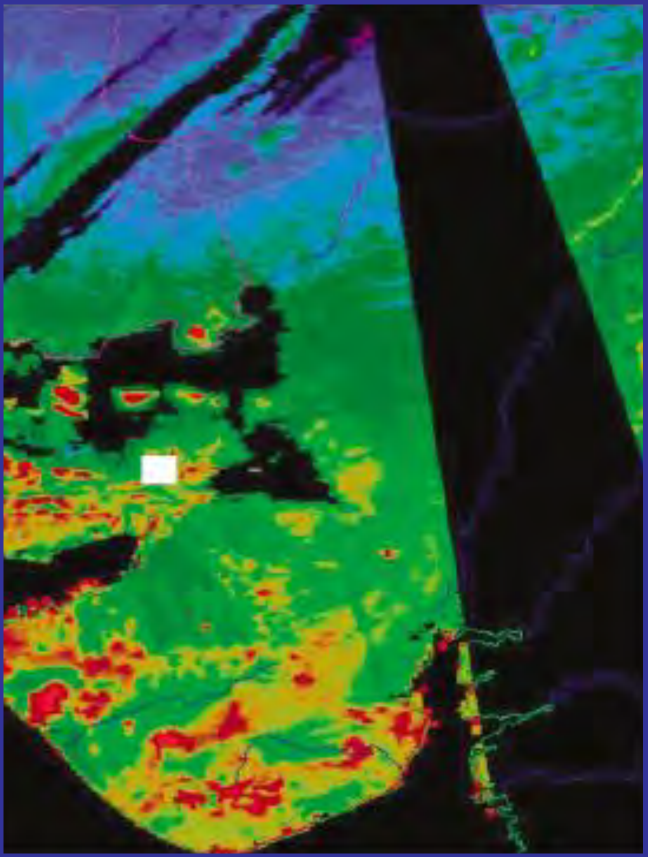

January 28, 2001

From IEEE SPECTRUM (Dec. 2005)

Theories on the Mechanisms Linking Crustal Activity to Electromagnetic Phenomena

Why are there electromagnetic anomalies associated with earthquakes?

Theories on the Mechanisms Linking Crustal Activity to Electromagnetic Phenomena

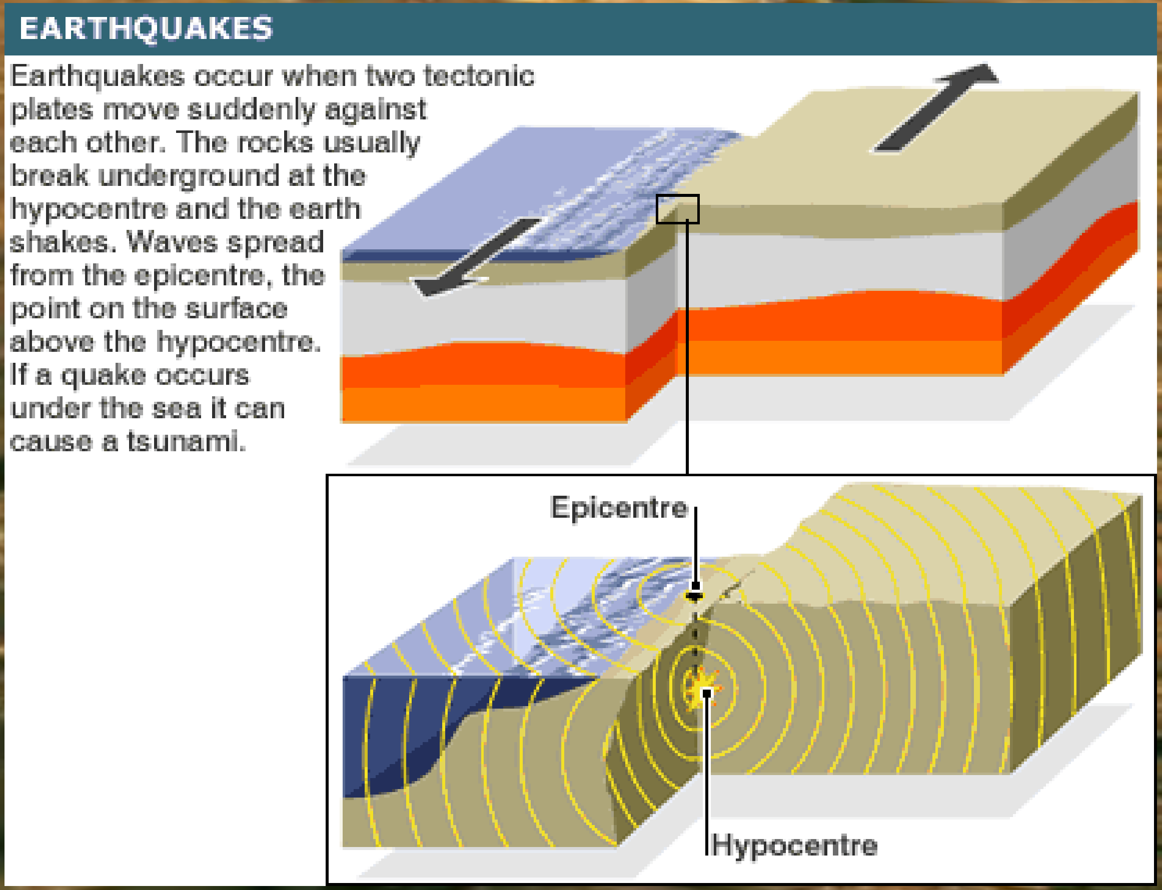

Theories on the Mechanisms Linking Crustal Activity to Electromagnetic Phenomena

Change in resistivity (conductivity) in the earthquake zone through piezoelectric effect

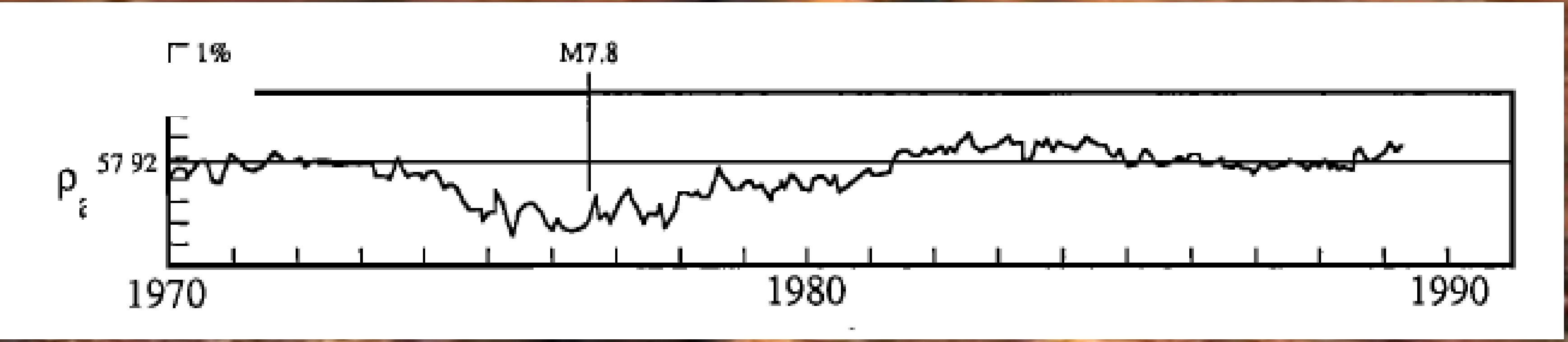

Resistivity change associated with the Tangshan (China) earthquake in 1976. Data were taken 80 km from the epicenter. (taken from Park et al., Rev Geophys 117, **31**, 1993 and Zhao et al., US-PRC Conference on Focused Earthquake Prediction Experiments, 1991.

Note: change in resistivity were not observed in other regions

Theories on the Mechanisms Linking Crustal Activity to Electromagnetic Phenomena

Microfracturing (Molchanov and Hayakawa Geophys. Res. Lett. 3091, 22, 1995)

- Microcracks develop due to the slow grinding or crust movement prior to an earthquake
- charges are created at the walls of crack openings due to instability of atoms induced by the grinding motion; flood of electrons is released due to the breaking of atomic/molecular bonds; holes (positive charge) are also created
- Electrons flow towards the earth's interior while holes flow towards the surface.

Theories on the Mechanisms Linking Crustal Activity to Electromagnetic Phenomena

Electrokinetic Theory **(H. Mizutani et al., Gephys. Res. Let. 365, *3*, 1976)**

occurs when an electrolyte flows through a capillary producing current

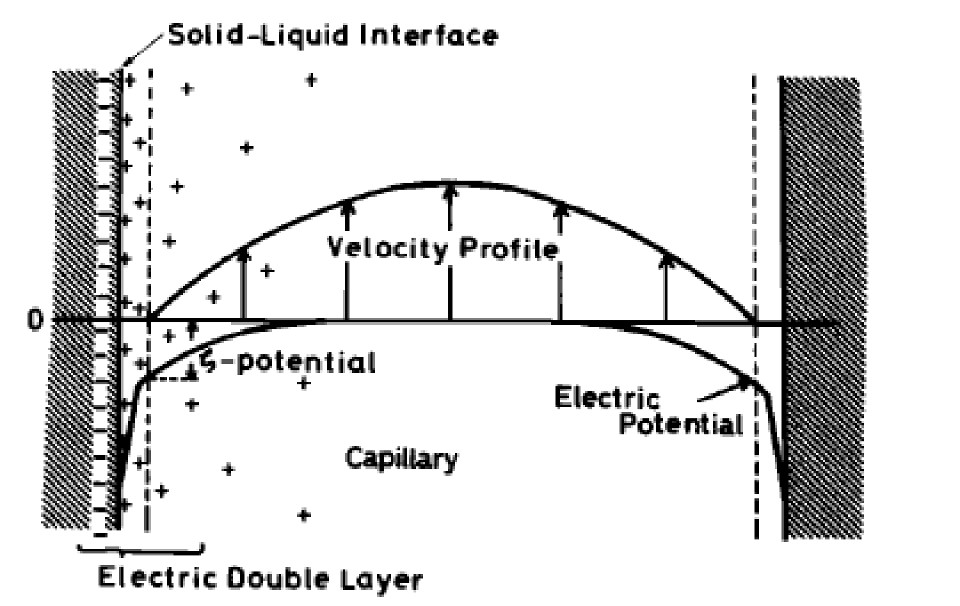

Taken from Mizutani et al.

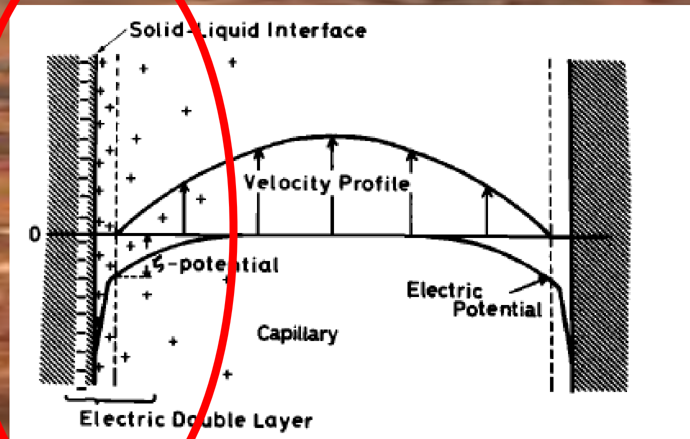

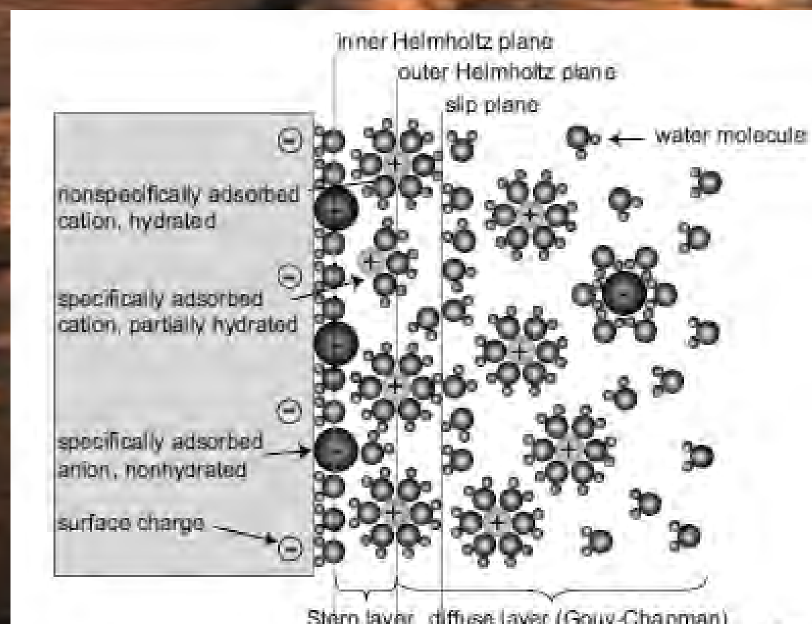

Taken from Rev. Mod. Phys. 840, *80*, 2008

Theories on the Mechanisms Linking Crustal Activity to Electromagnetic Phenomena

a porous medium can be considered as a bundle of capillaries (Scheidegger 1974)

$$-\vec{j} = \phi\sigma\vec{\nabla}V - \frac{\phi\varepsilon\varsigma}{\eta}\vec{\nabla}P$$

$$-\vec{v} = -\frac{\phi\varepsilon\varsigma}{\eta}\vec{\nabla}V + \frac{k}{\eta}\vec{\nabla}P$$

Byerlee (*Geology*, **21**,303-306, 1993) earlier proposed that through silica deposition results to the formation of sealed compartments of various sizes and porosities.

Unsteady flow of ionized groundwater due to the rupture of sealed compartments. This unsteady flow produces transient electric and magnetic fields through electrokinetic signal (Fenoglio et al. *J. Geophys. Res.*, 100, B7, 12951-12958, 1995).

Theories on the Mechanisms Linking Crustal Activity to Electromagnetic Phenomena

Semiconductor Effect (Freund IEEE Spectrum, 2005)

This asserts that a flood of electrons and holes is released due to the breaking of atomic/molecular bonds brought about by this deformation or breakage. Indeed, rock crushing experiments showed that sundering of oxygen-oxygen bonds in minerals of fracturing rocks could produce electron-hole pairs. Electrons may manage to flow towards the mantle while holes flow towards the ground making it positively charged.

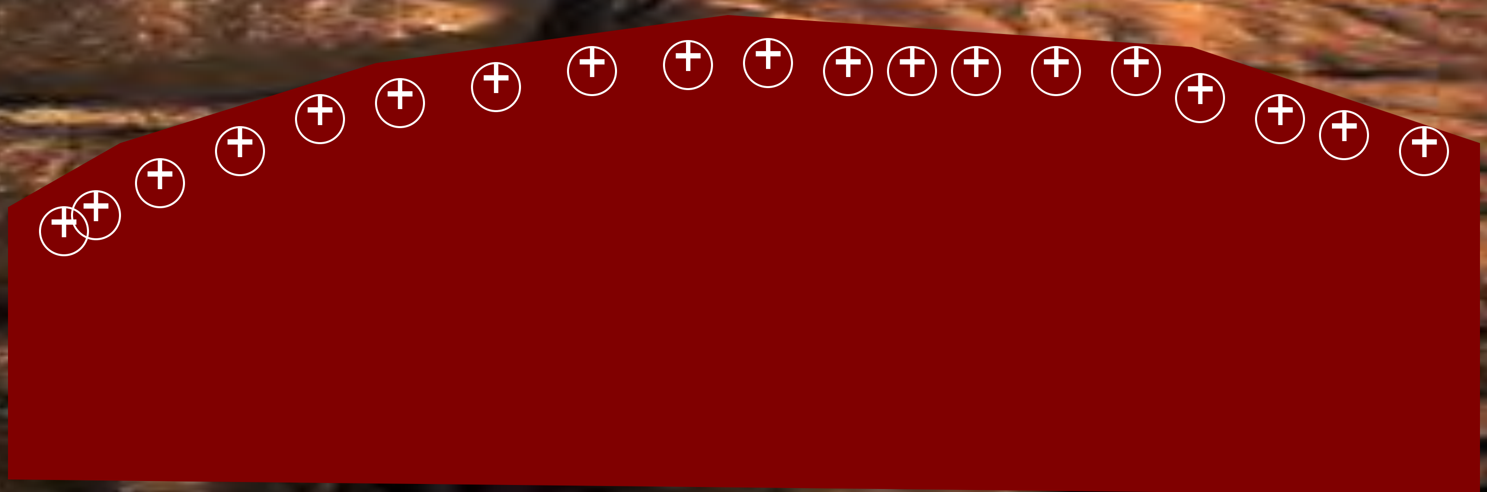

Pre-earthquake signals: Underlying physical processes. Freund, F. 2011, Journal of Asian Earth Sciences, pp. 383-400.

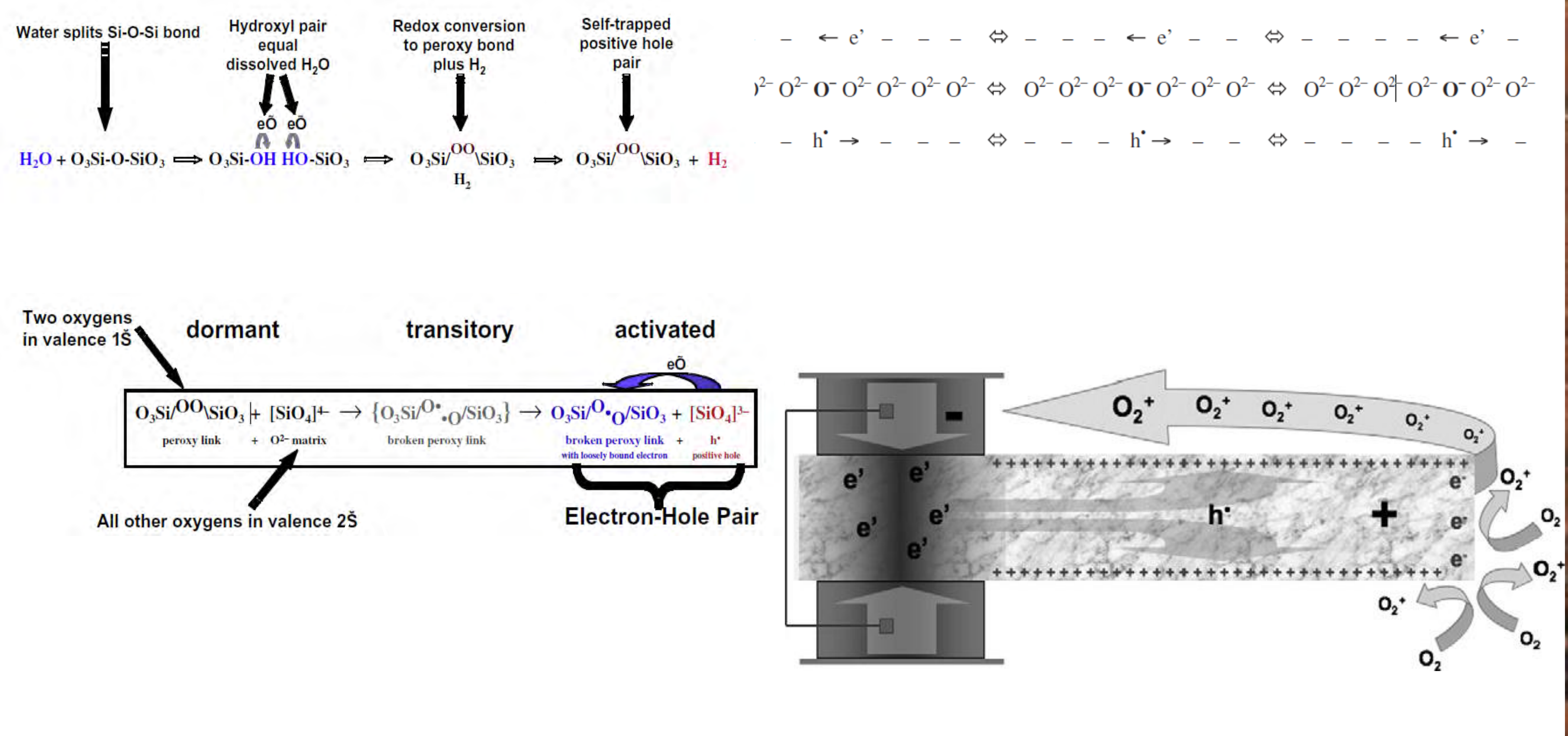

Lithosphere-Atmosphere-Ionosphere Coupling (LAIC) Model

by S. Pulinets and D. Ouzounov

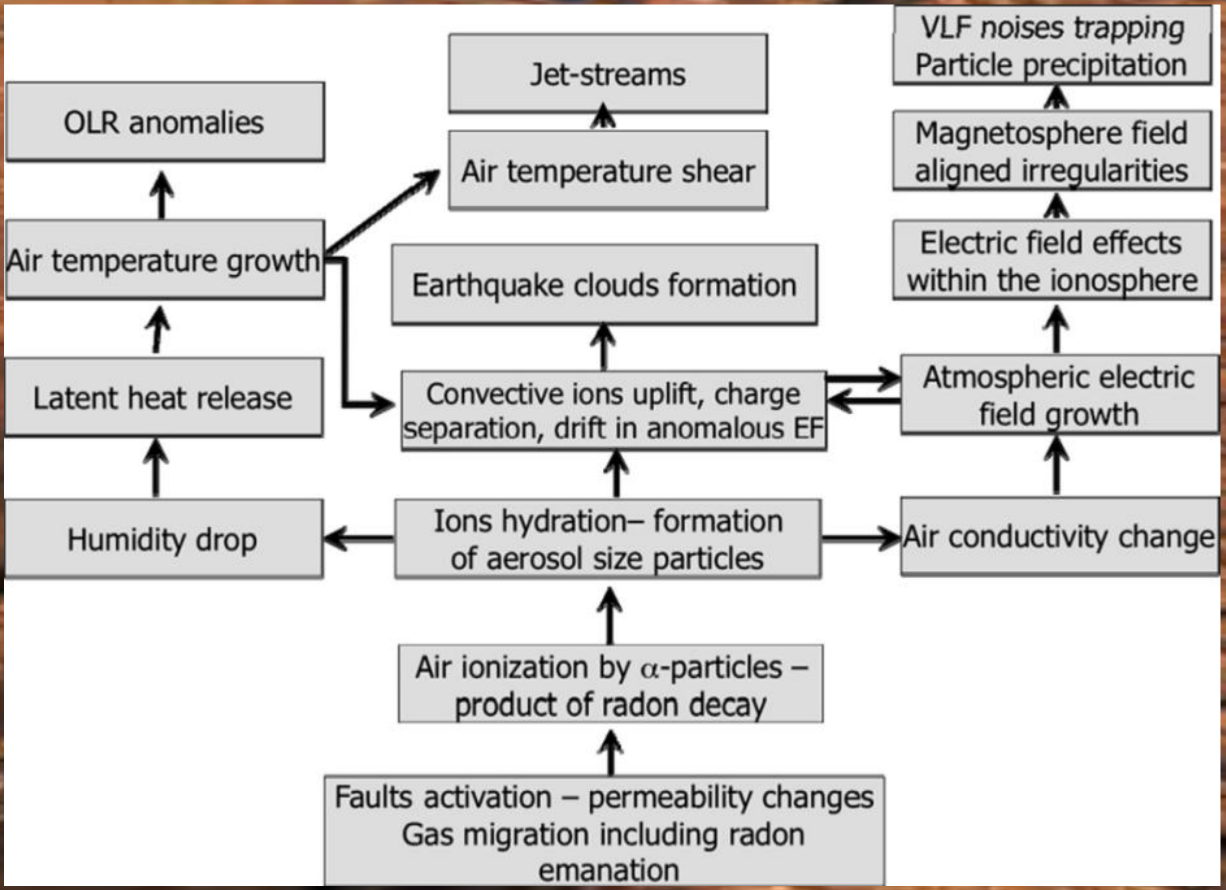

Lithosphere-Atmosphere-Ionosphere Coupling (LAIC) model - An unified concept for earthquake precursors validation. D.Ouzounov, S. Pulinets and. 41, s.l. : Journal of Asian Earth Sciences, 2011, pp. 371-382

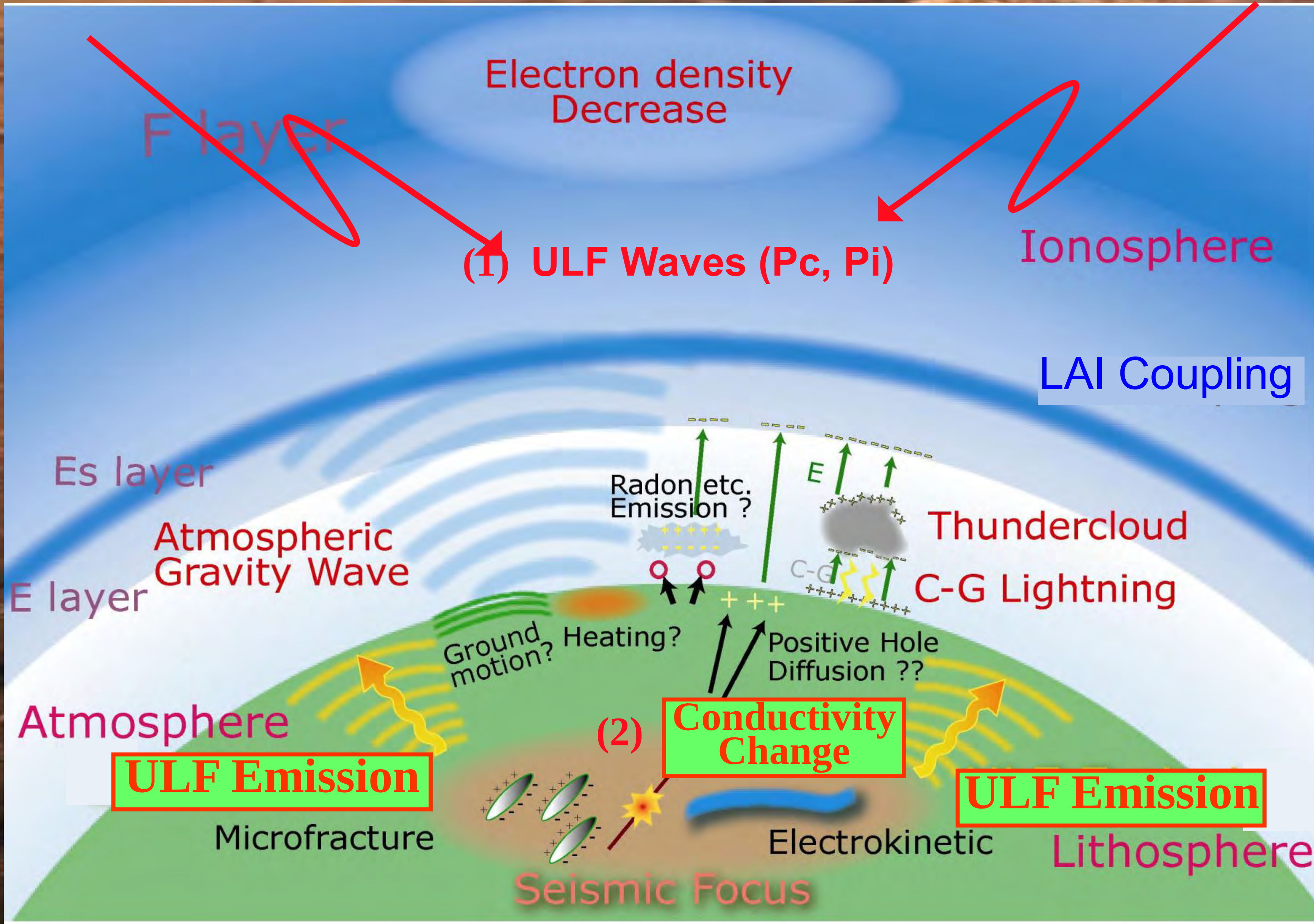

Electron density
Decrease
F layer
(1) ULF Waves (Pc, Pi)
Ionosphere
LAI Coupling
Es layer
Radon etc.
Emission ?
E
Thundercloud
Atmospheric
Gravity Wave
C-G
C-G Lightning
E layer
Ground
motion?
Heating?
Positive Hole
Diffusion ??
Atmosphere
(2)
Conductivity
Change
ULF Emission
ULF Emission
Microfracture
Electrokinetic
Lithosphere
Seismic Focus

Contents lists available at ScienceDirect

Physics and Chemistry of the Earth

journal homepage: www.elsevier.com/locate/pce

A new ULF wave analysis for Seismo-Electromagnetics using CPMN/MAGDAS data

K. Yumoto [a,b,*], S. Ikemoto [b], M.G. Cardinal [b], M. Hayakawa [c], K. Hattori [d], J.Y. Liu [e], S. Saroso [f], M. Ruhimat [f], M. Husni [g], D. Widarto [h], E. Ramos [i], D. McNamara [i], R.E. Otadoy [j], G. Yumul [k], R. Ebora [k], N. Servando [k]

Table 1. The classification of geomagnetic pulsations.

	Pulsation Classes						
	Continuous pulsations					Irregular pulsations	
	Pc1	Pc2	Pc3	Pc4	Pc5	Pi1	Pi2
T	0.2–5s	5–10s	10–45s	45–150s	150–600s	1–40s	40–150s
f	0.2–5Hz	0.1–0.2Hz	22–100mHz	7–22mHz	2–7mHz	0.025–1Hz	2–25mHz

ULF wave amplitudes observed on the ground show seasonal, local time, and latitudinal variations (cf. Yumoto, 1986), which are a function of parameters in the solar wind, magnetoshere, ionosphere, and lithosphere, and can be expressed in the following equation (Chi et al., 1996)

$$A = B\, f(LT)\, c$$

where A, B, f, and c are ULF amplitude observed on the ground, parameter of source wave in the solar wind and/or magnetosphere, local time dependence in the ionosphere, and amplification factor in the lithosphere, respectively.

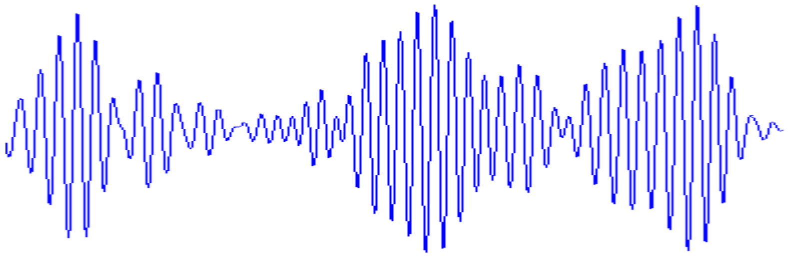

Pc3

ULF anomaly associated with the change in geoconductivity, precursory feature can be extracted by the following (Yumoto et al. 2007):

1. calculation of the polarization ratio, the power ratio between the horizontal (H) to the vertical (Z) components of the Pc 3-4 magnetic pulsations observed at a station near the epicenter;

2. calculation of the H- and Z- power ratios of Pc3 magnetic pulsations observed at station near the epicenter to the reference station remote from the epicenter;

3. calculation of the power ratios of each day to the one-year averaged data at a station close to the epicenter.

Since changes in the geomagnetic field are influenced more by space sources than by lithospheric processes, the above techniques will hopefully filter out the influence of the former.

Theories on the Mechanisms Linking Crustal Activity to Electromagnetic Phenomena

Changing geoelectric conductivity (causes change in polarization and power)

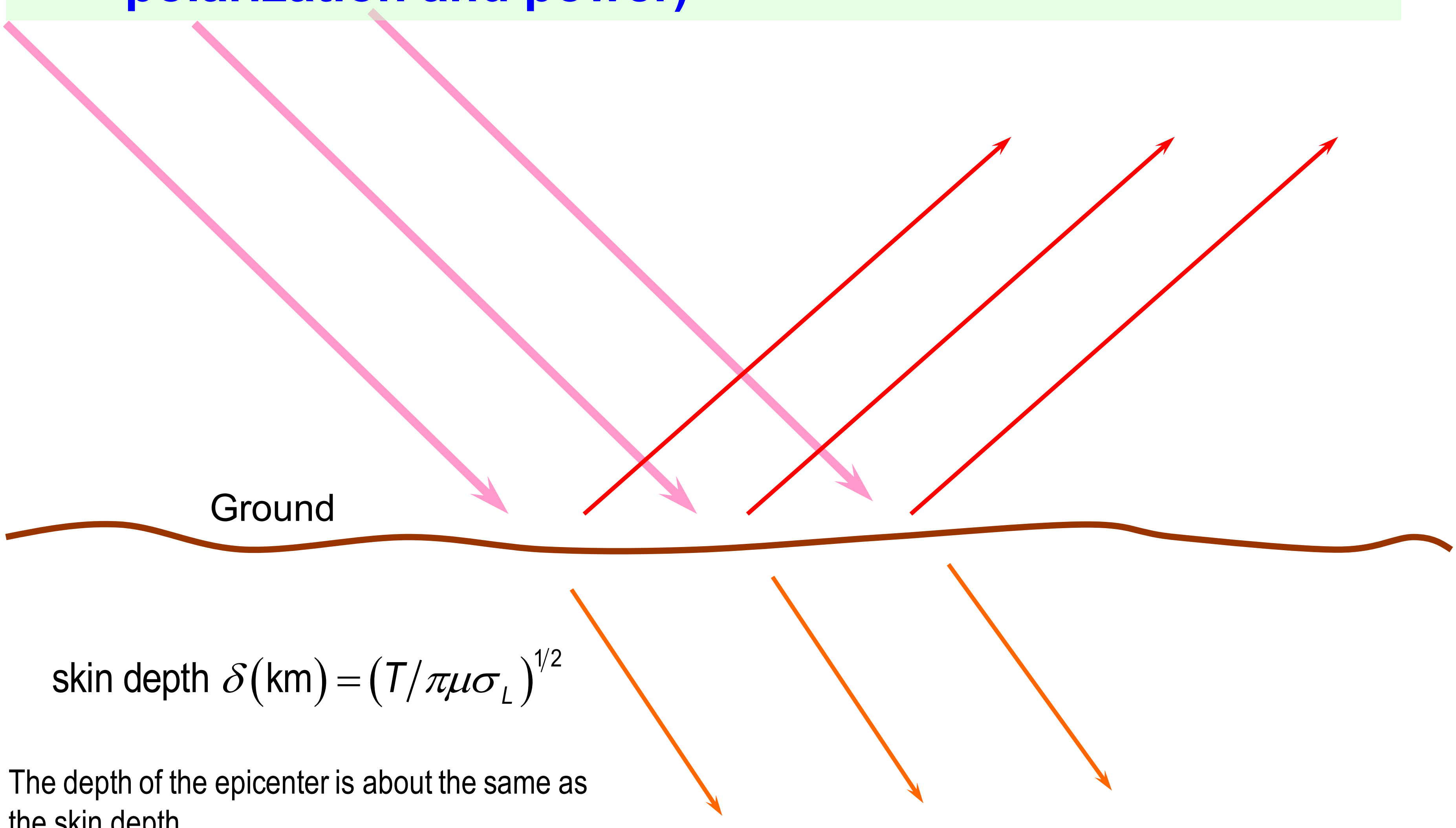

skin depth $\delta(\text{km}) = \left(T/\pi\mu\sigma_L\right)^{1/2}$

The depth of the epicenter is about the same as the skin depth

ULF WAVE AND LITHOSPHERE-ATMOSPHERE-SPACE ENVIRONMENT COUPLING

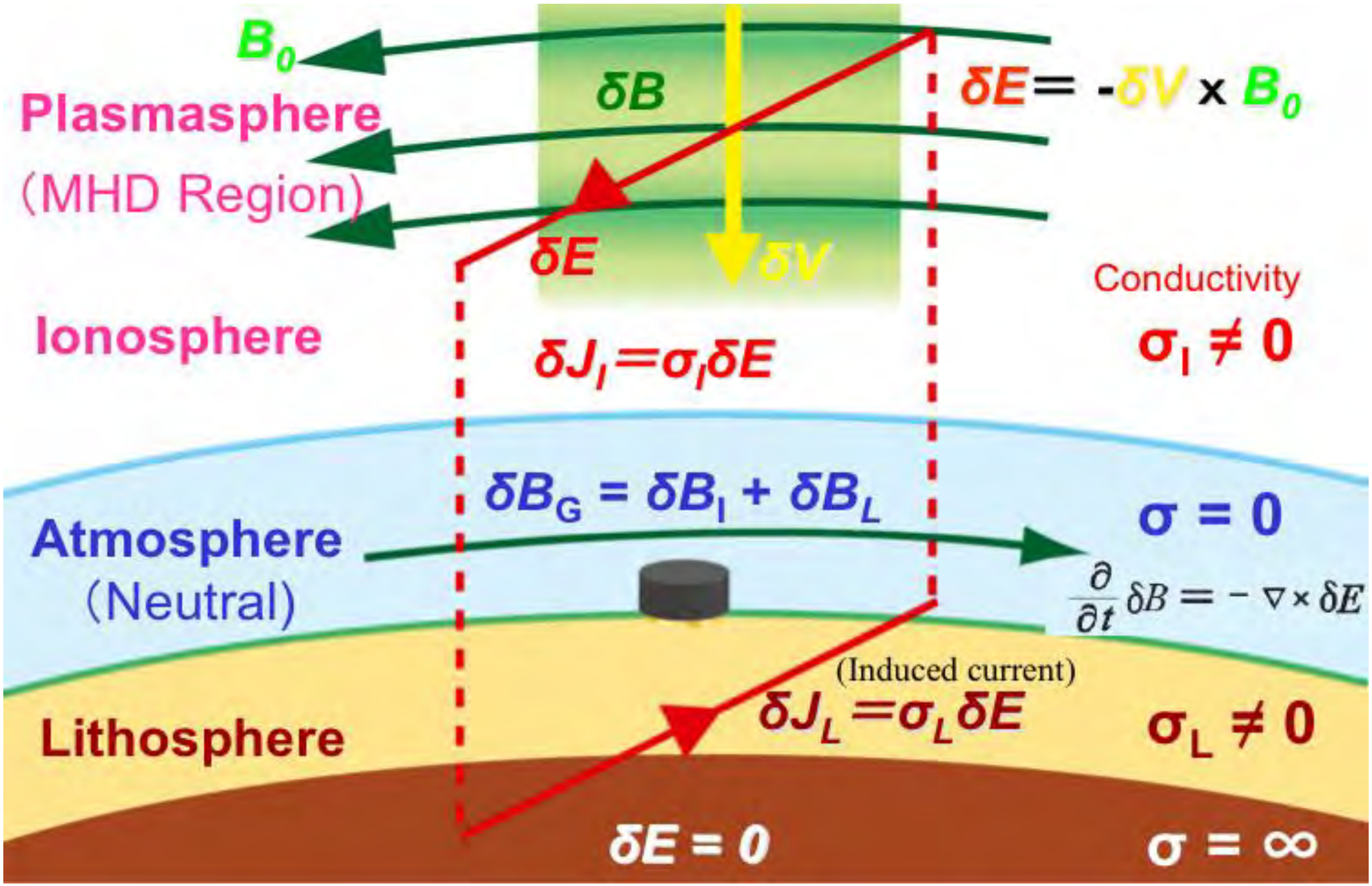

Electromagnetic coupling of ULF waves in the plasmasphere-ionosphere-atmosphere-lithosphere near the equator (Yumoto, McNamara, Otadoy, et al., 2007)

MAGDAS III Project for Litho-Space Weather in Asia

K. Yumoto[1,2], M.G. Cardinal[2], K. Hattori[3], M. Hayakawa[4], J.Y. Liu[5], P. Harjadi[6],
B. S. Tejasukmana[7], H. Harjono[8], and MAGDAS Group

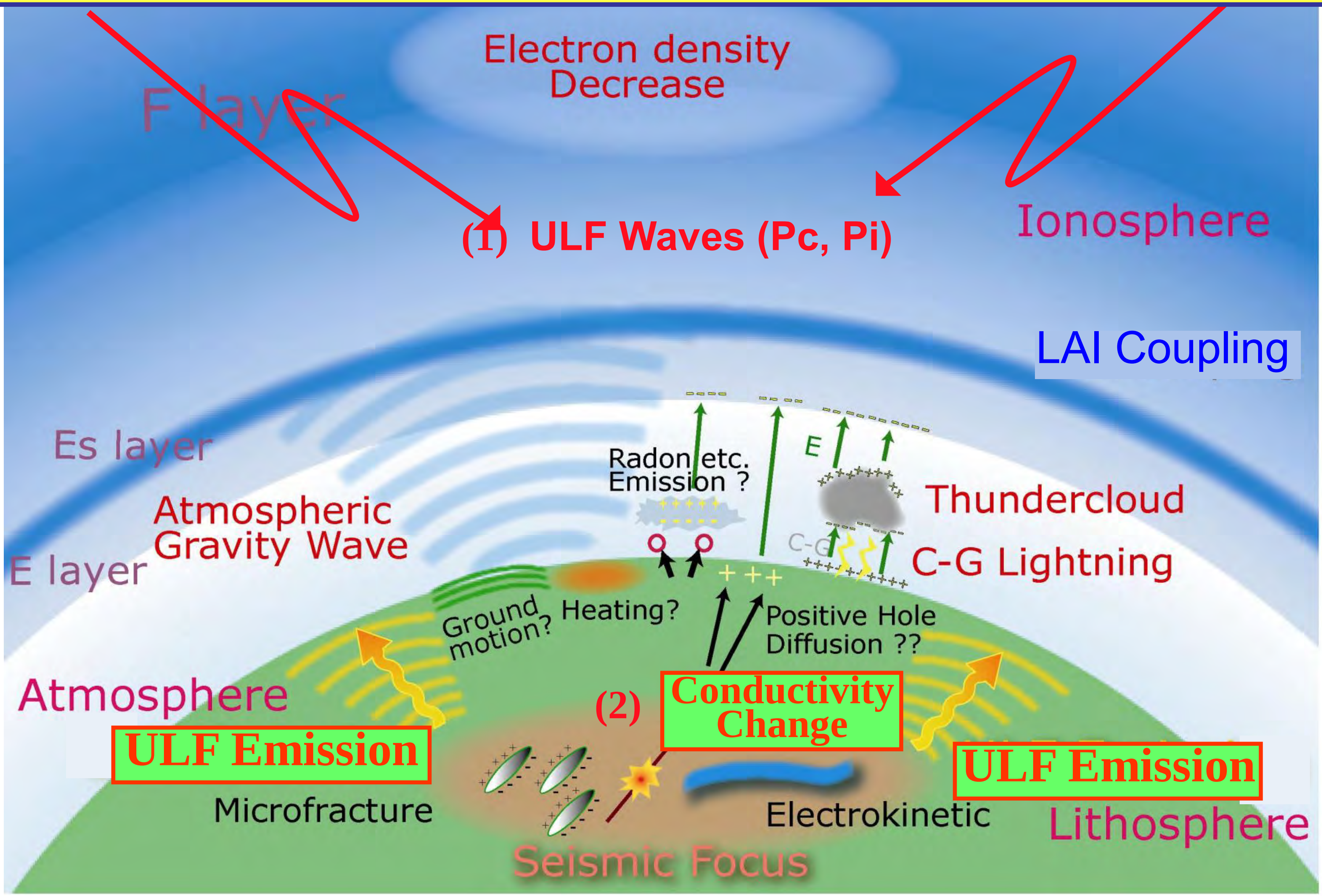

CASE STUDY

Moderately large earthquake occurred at Kushiro (Geo. Lat. = 42.95N, Geo. Long. = 143.91E) in Hokkaido, Japan, at 17h 59m UT on May 12, 1999, magnitude was 6.4 and its depth was about 104 km.

At that time magnetic observations were operated at Rikubetsu (RIK: 43.5N, 143.8E) and Moshiri (MSR: 44.37N, 142.27E) stations, which belong to the Solar Terrestrial Environment Laboratory, Nagoya University.

The distance between the epicenter of earthquake and RIK and MSR stations were 61 km and 205 km, respectively.

EQ's magnitude and distance between the epicenter and the observatory where ULF anomaly were observed (courtesy of Hattori et al., 2006)

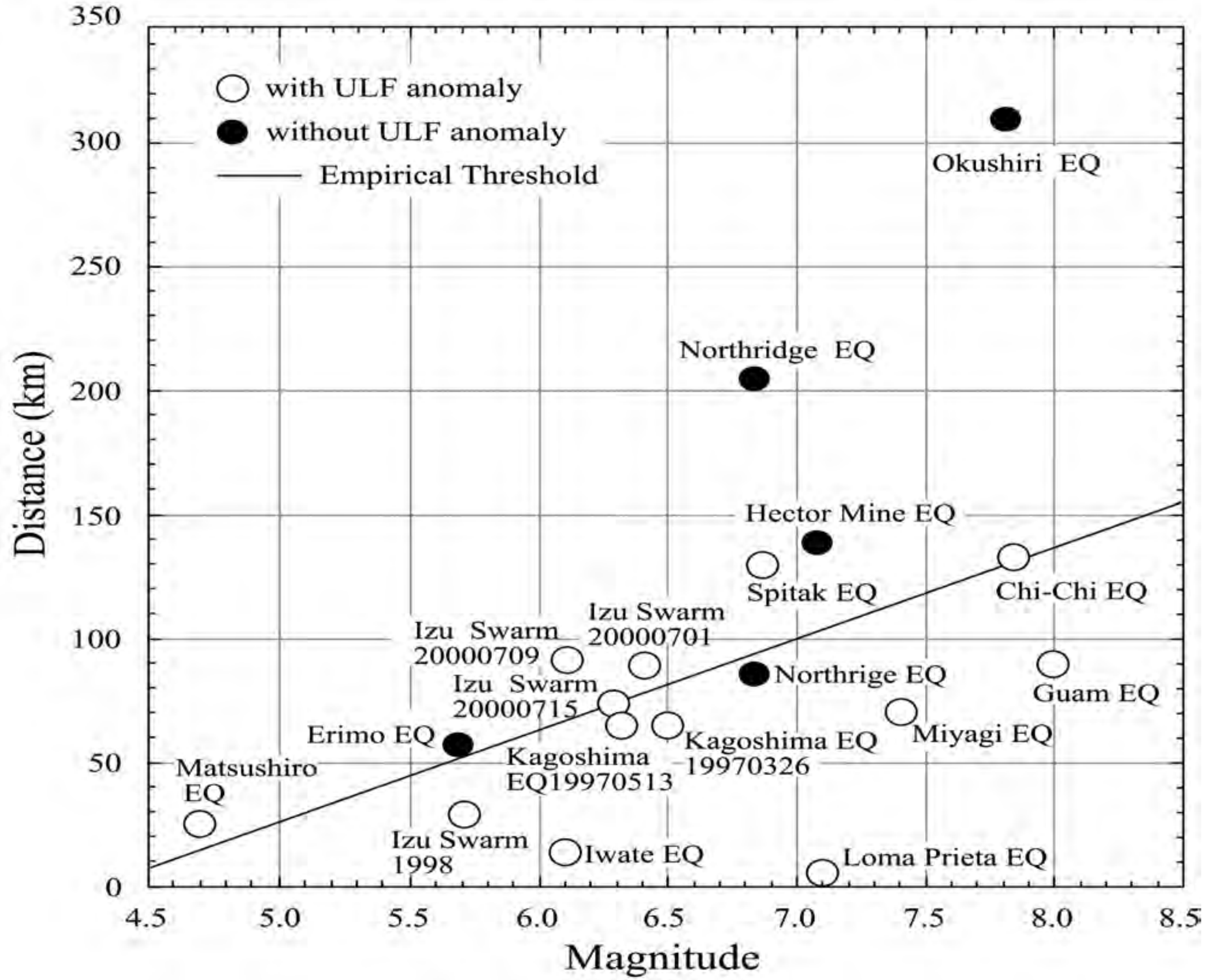

2012 M6.9 Negros Earthquake

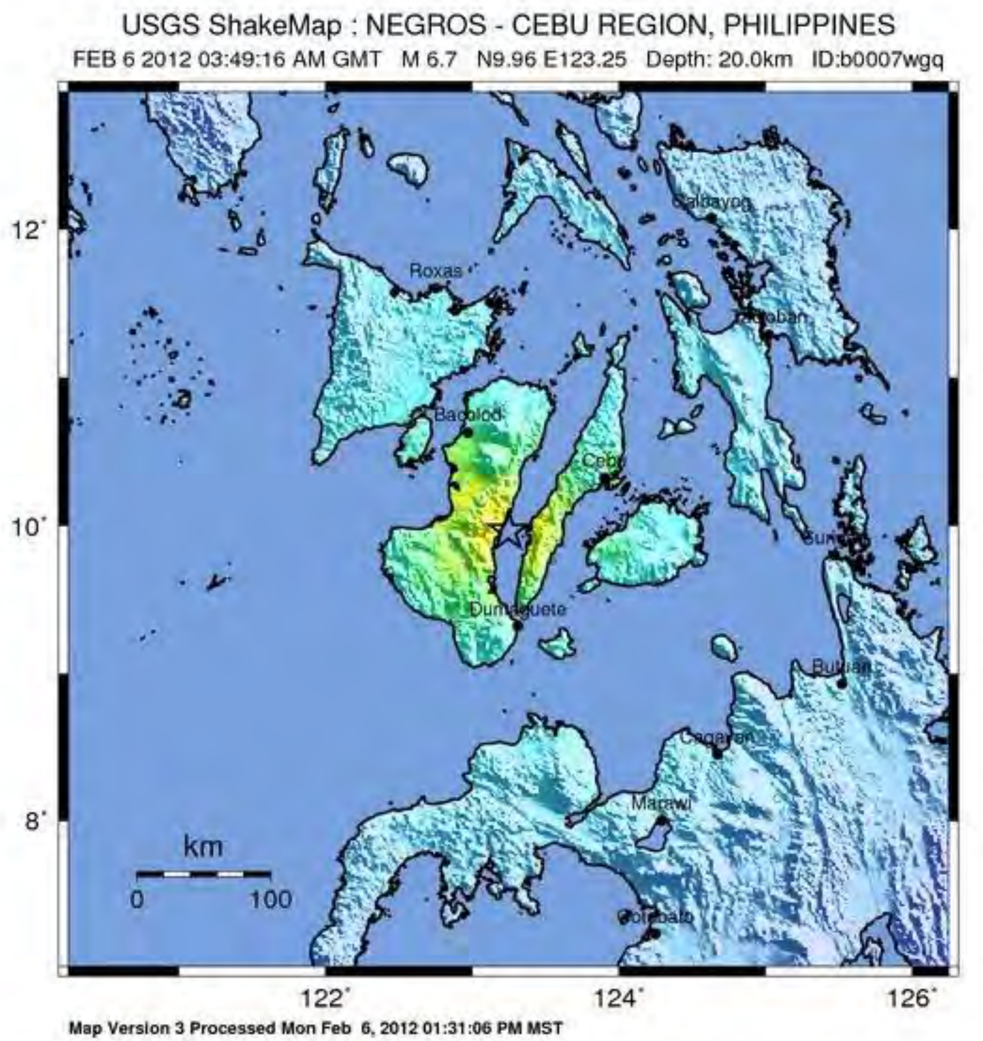

PERCEIVED SHAKING	Not felt	Weak	Light	Moderate	Strong	Very strong	Severe	Violent	Extreme
POTENTIAL DAMAGE	none	none	none	Very light	Light	Moderate	Mod./Heavy	Heavy	Very Heavy
PEAK ACC.(%g)	<0.03	0.3	2.8	6.2	12	22	40	75	>139
PEAK VEL.(cm/s)	<0.01	0.1	1.4	4.7	9.6	20	41	86	>178
INSTRUMENTAL INTENSITY	I	II-III	IV	V	VI	VII	VIII	IX	X+

Scale based upon Worden et al. (2011)

- MAGDAS/CPMN – Z/H polarization pc3 power ratio

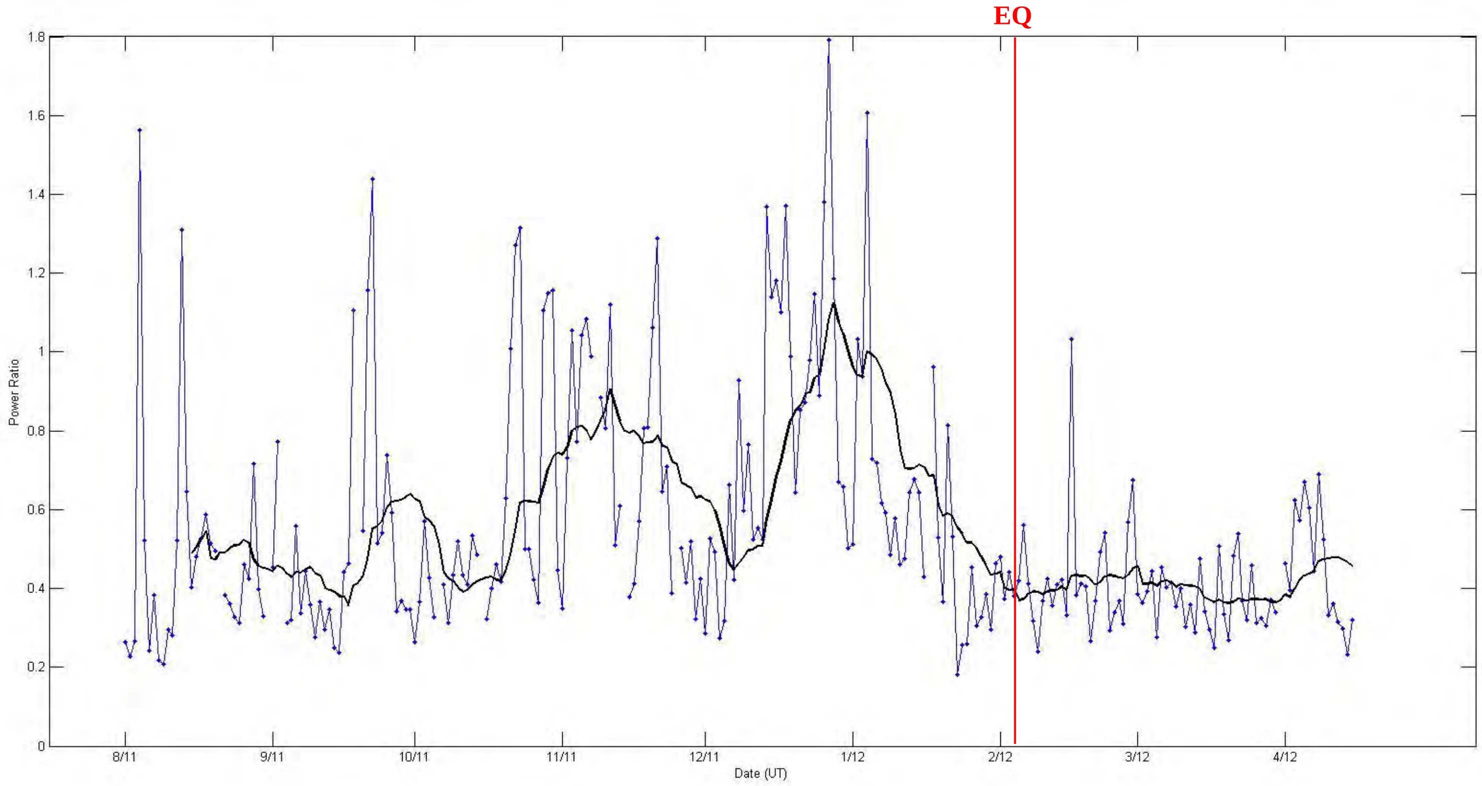

Z/H pc3 power ratio for CEB station for the M6.9 Negros Oriental Earthquake

- MAGDAS/CPMN – CEB/DAV H-component pc3 power ratio

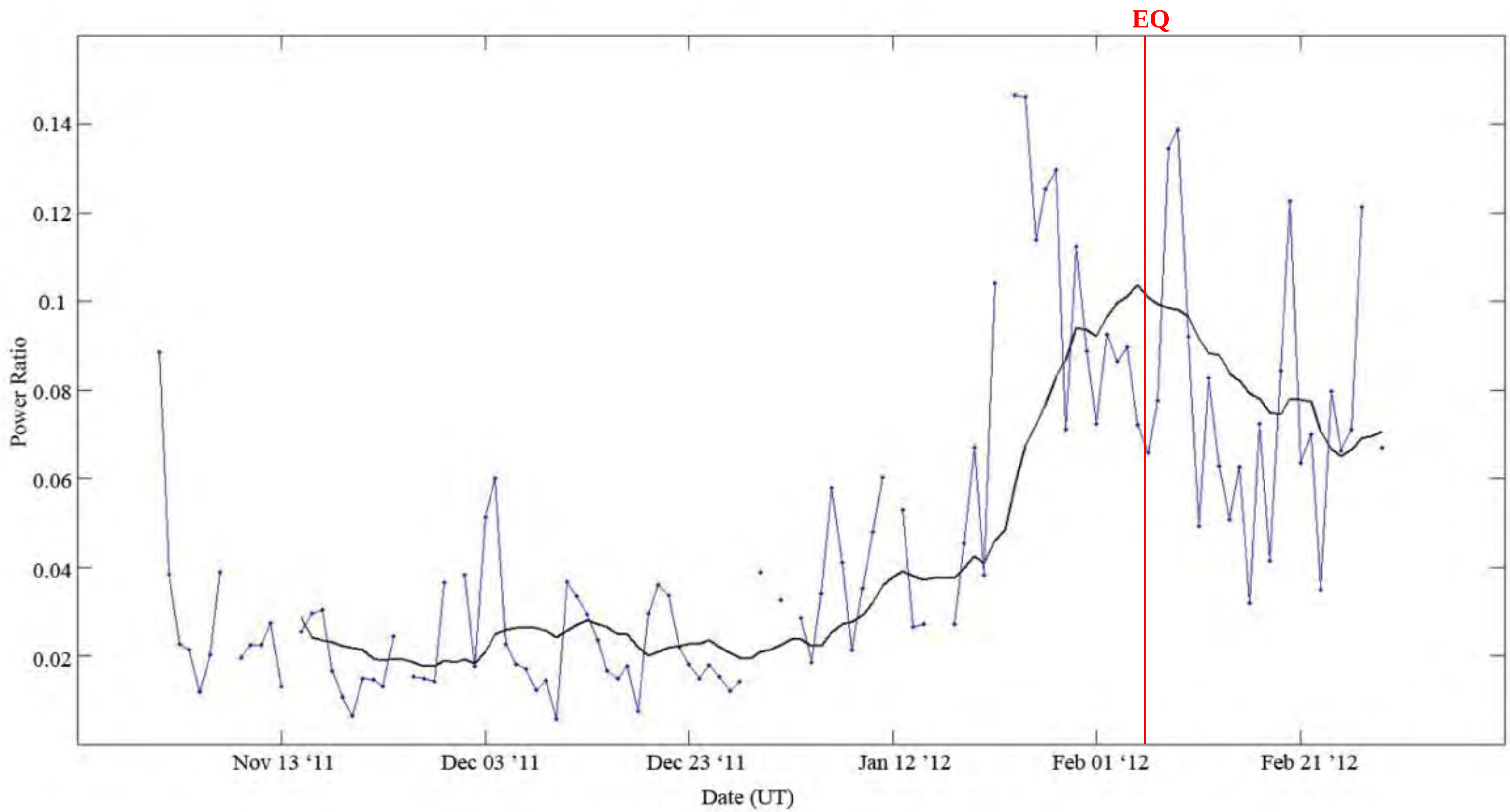

H-component pc3 power ratio as a function of Date in UT between CEB and DAV stations

- MAGDAS/CPMN – CEB/MUT H-component pc3 power ratio

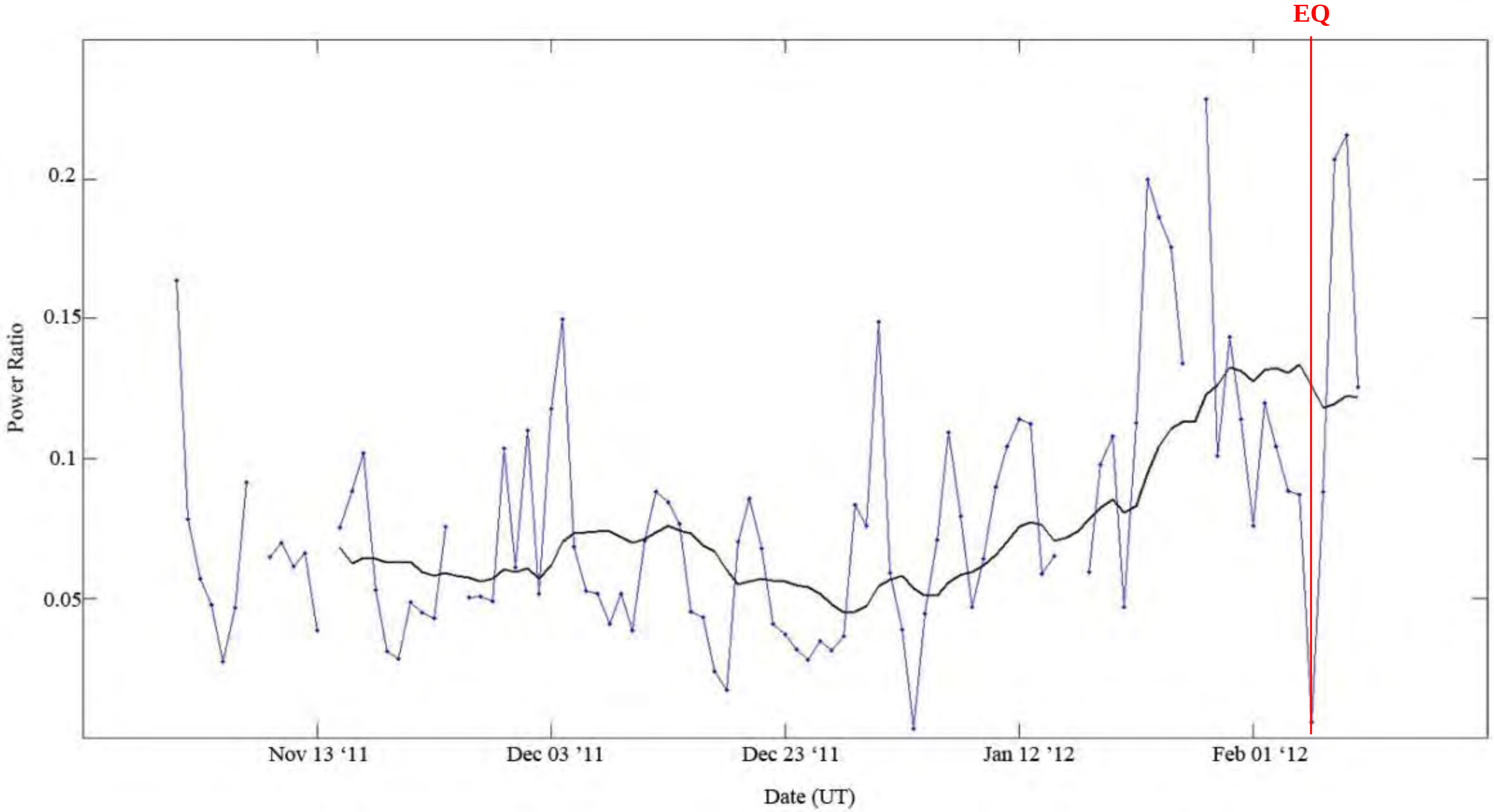

H-component pc3 power ratio as a function of Date in UT between CEB and MUT stations

- MAGDAS/CPMN – One-day to One-year average H-component pc3 power ratio

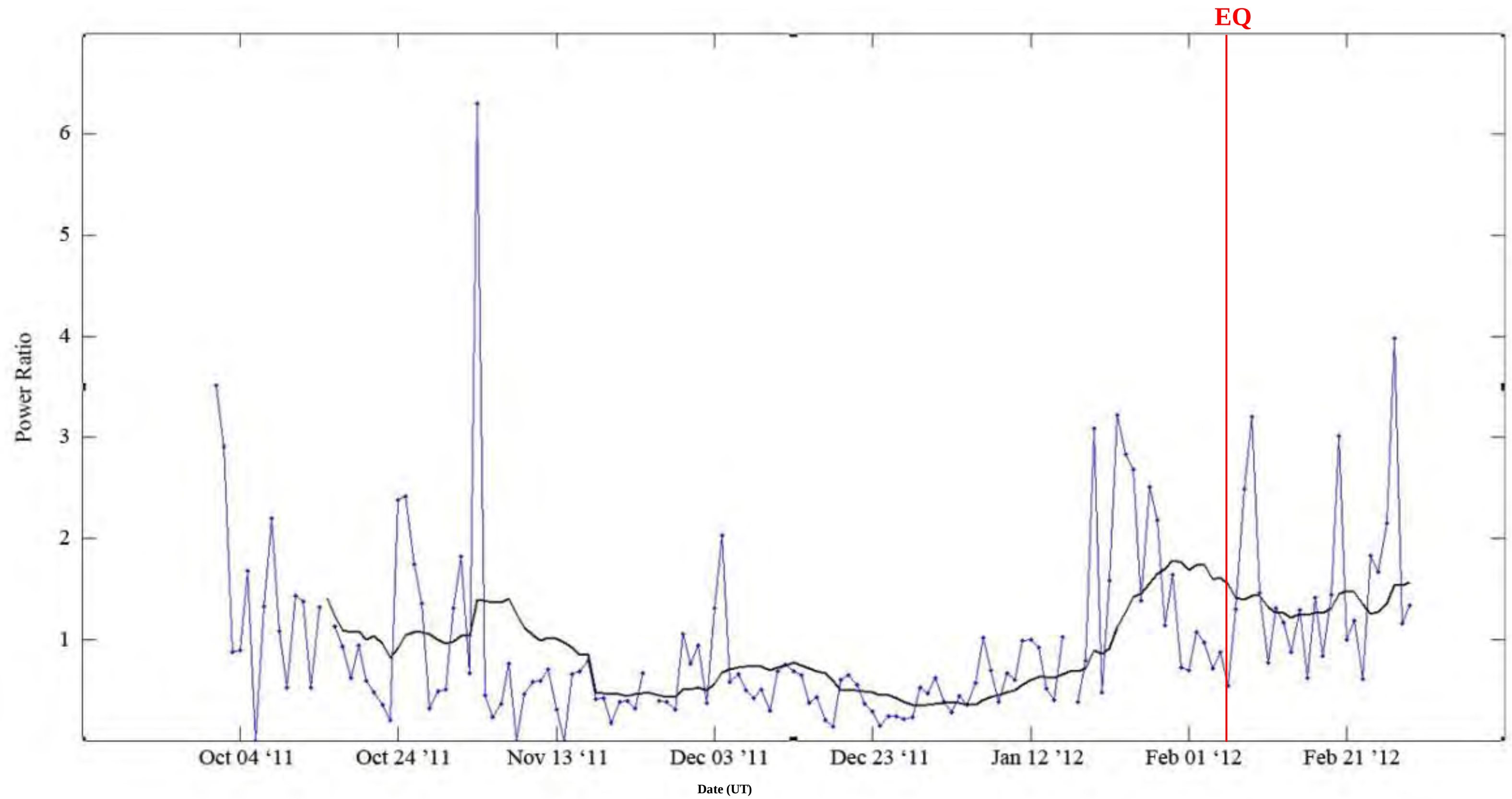

H-component pc3 power ratio as a function of Date in UT between CEB and MUT stations

Ionospheric Perturbations – Electron Density Anomalies

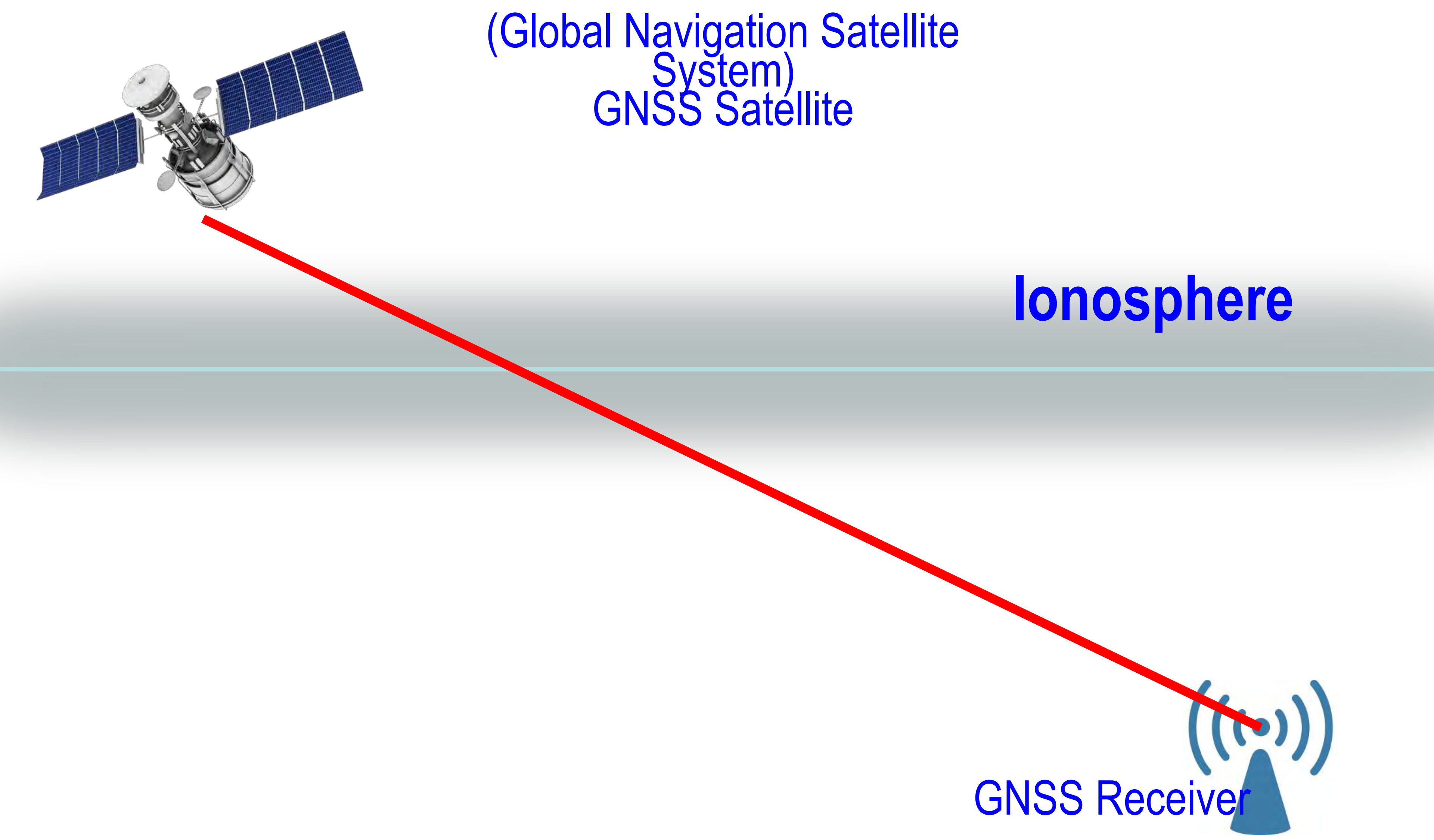

Ionospheric Perturbations – Electron Density Anomalies

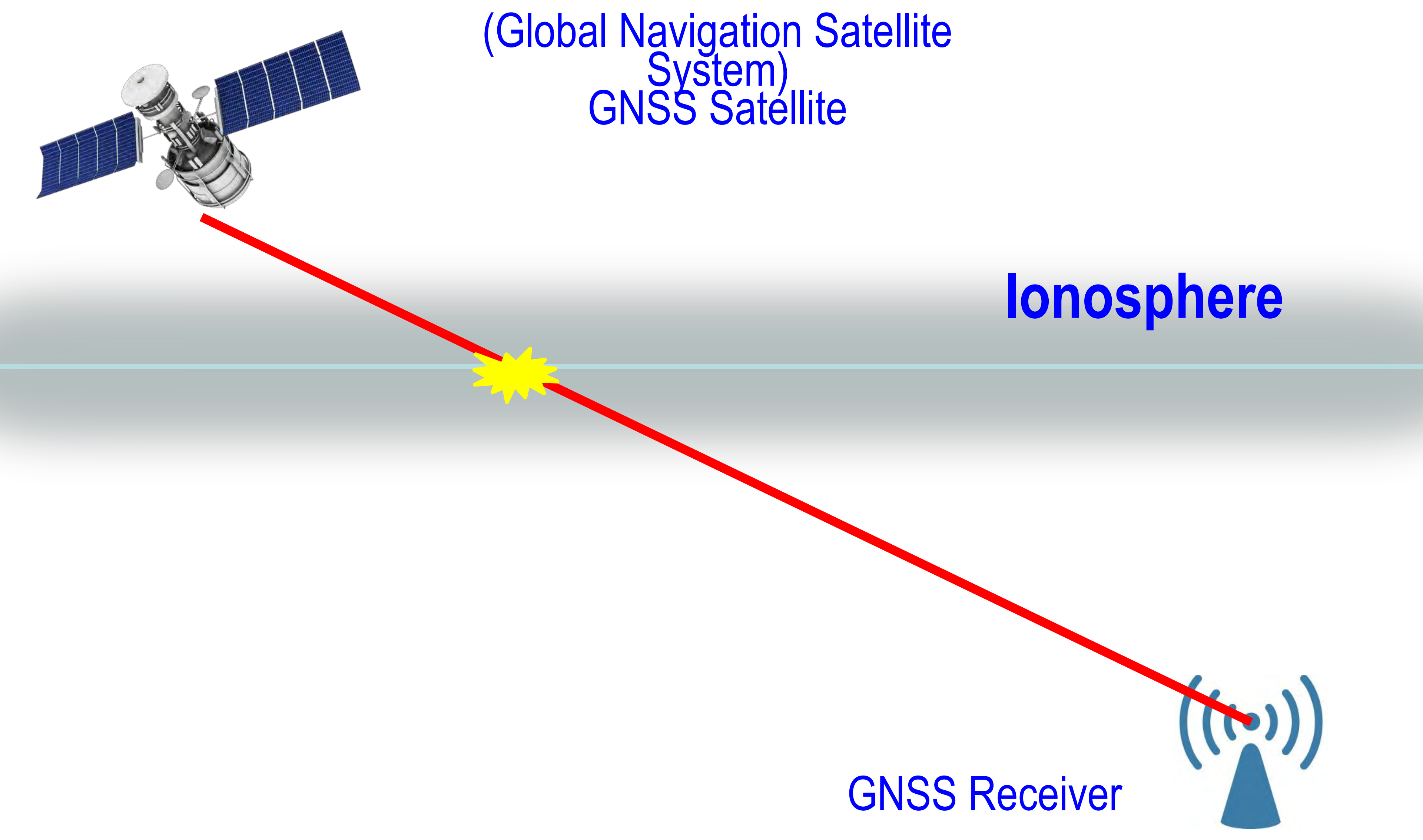

NAVSTAR (Navigation Satellite Timing and Ranging)

GPS (Global Positioning System)

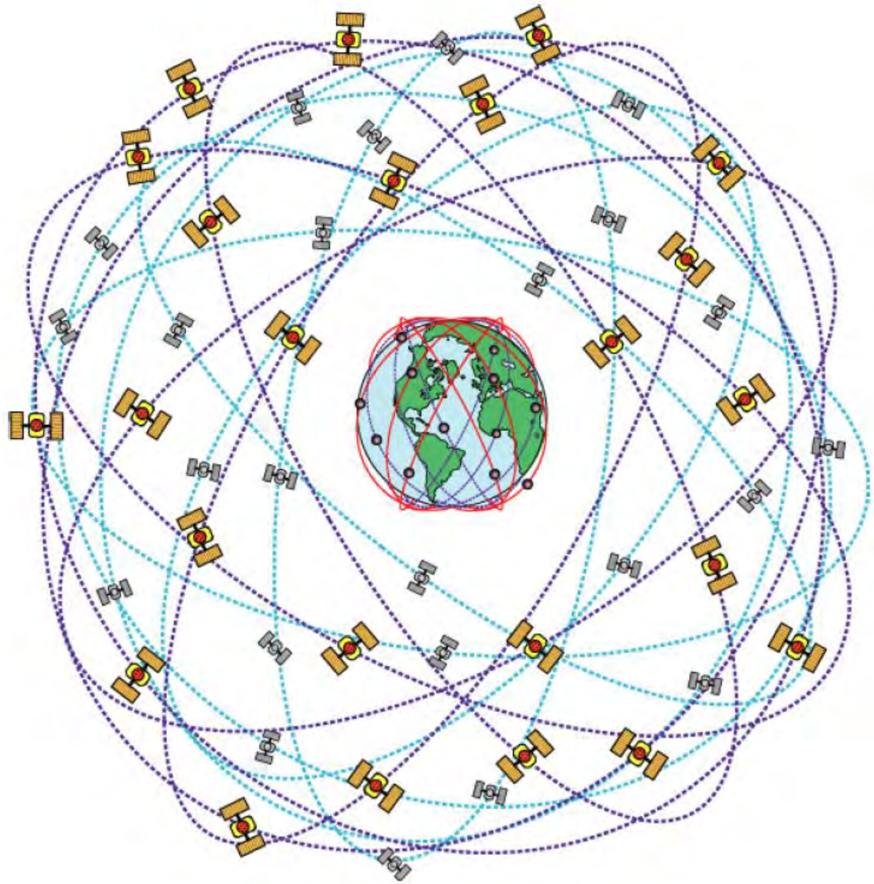

GNSS satellites

- GPS (US)
- Galileo (EU)
- GLONASS (Russia)
- QZ (Japan)

GPS Frequencies:
L1: 1.57542GHz
L2: 1.22760GHz

Radio wave delay = delay by distance
+ delay caused by troposphere(water vapor and temp.)
+ delay caused by ionosphere(Total Electron Content)

$$-d_p = d_g = \frac{40.3T}{f^2}$$

d_p, d_g : delay of phase and group velocities
T: Total Electron Content (TEC)
f: radio frequency(L1 and L2)

1TECU ~ 16cm

Ionospheric Perturbations – GPS-TEC

GPS-TEC – Global Positioning System – Total Electron Content

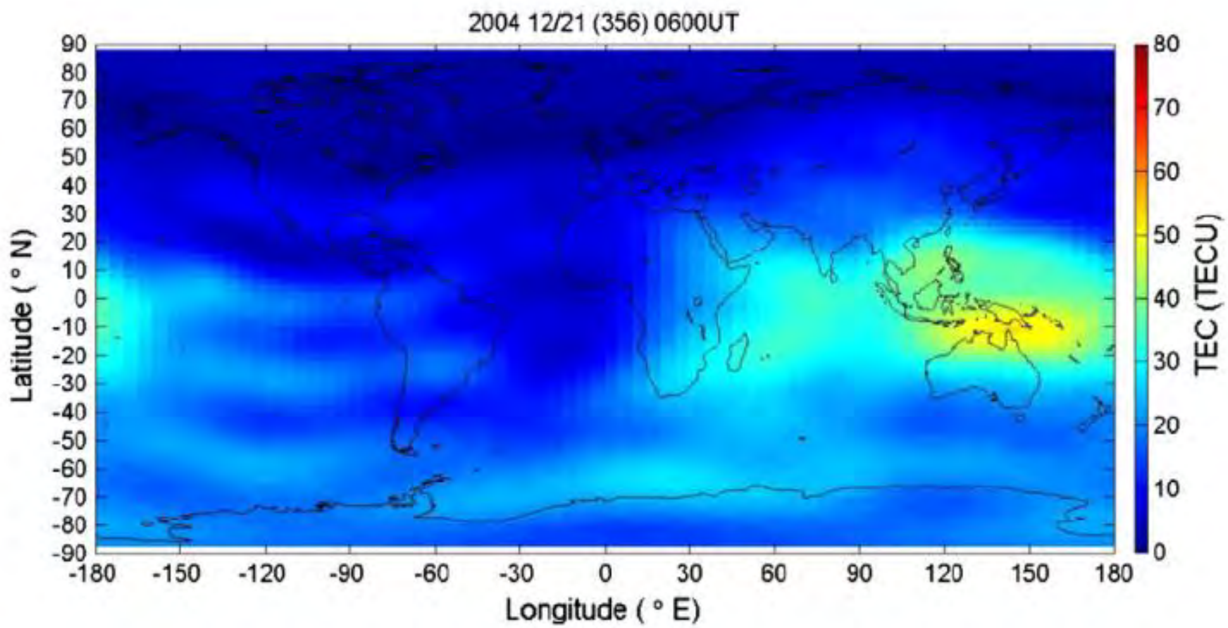

A typical GIM TEC. The observation was conducted at 06:00UT on 21 December 2004 which is day 5 before the Sumatra earthquake.

CODE – Center for Orbit Determination in Europe

- Over 200 GPS receivers worldwide
- 2-h GIM(Global Ionosphere Maps) resolution

GPS-TEC – Global Positioning System – Total Electron Content

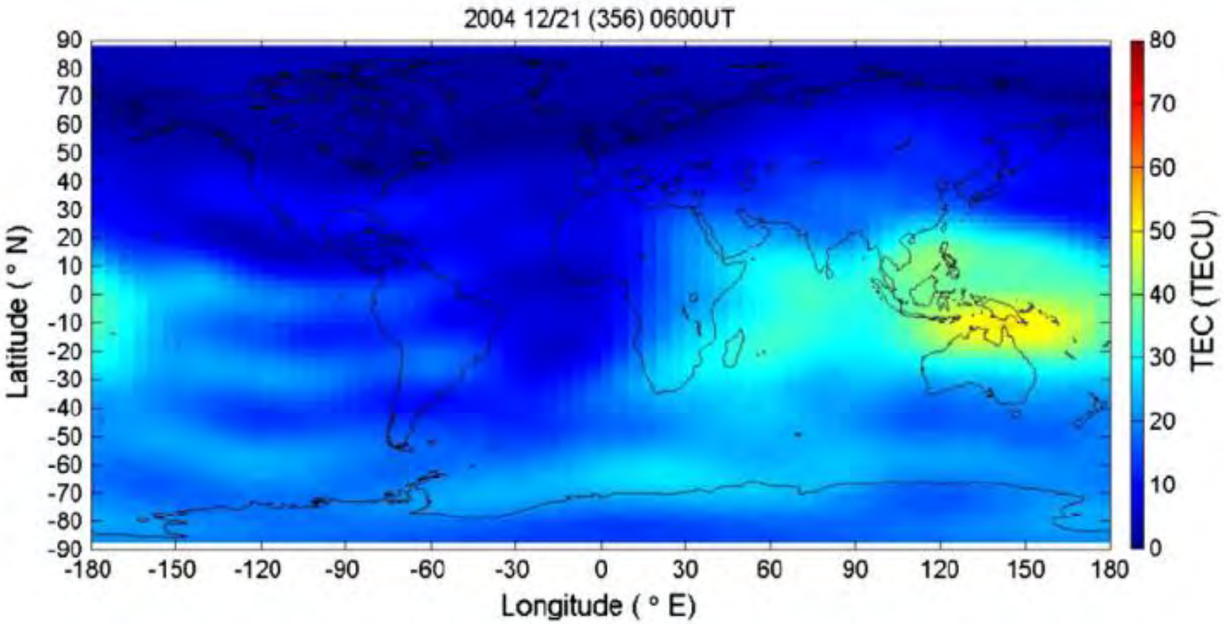

A typical GIM TEC. The observation was conducted at 06:00UT on 21 December 2004 which is day 5 before the Sumatra earthquake.

- Normalized GIM-TEC by S. Kon et. al.
- Quartile Based Method by Liu et. al.

Ionospheric Perturbations – GPS-TEC

$$[\mathrm{GIM-TEC}^*(t)] = \frac{[\mathrm{GIM-TEC}(t)] - [\overline{\mathrm{GIM-TEC}(t)}]}{\sigma(t)}$$

Mean of previous 15 days

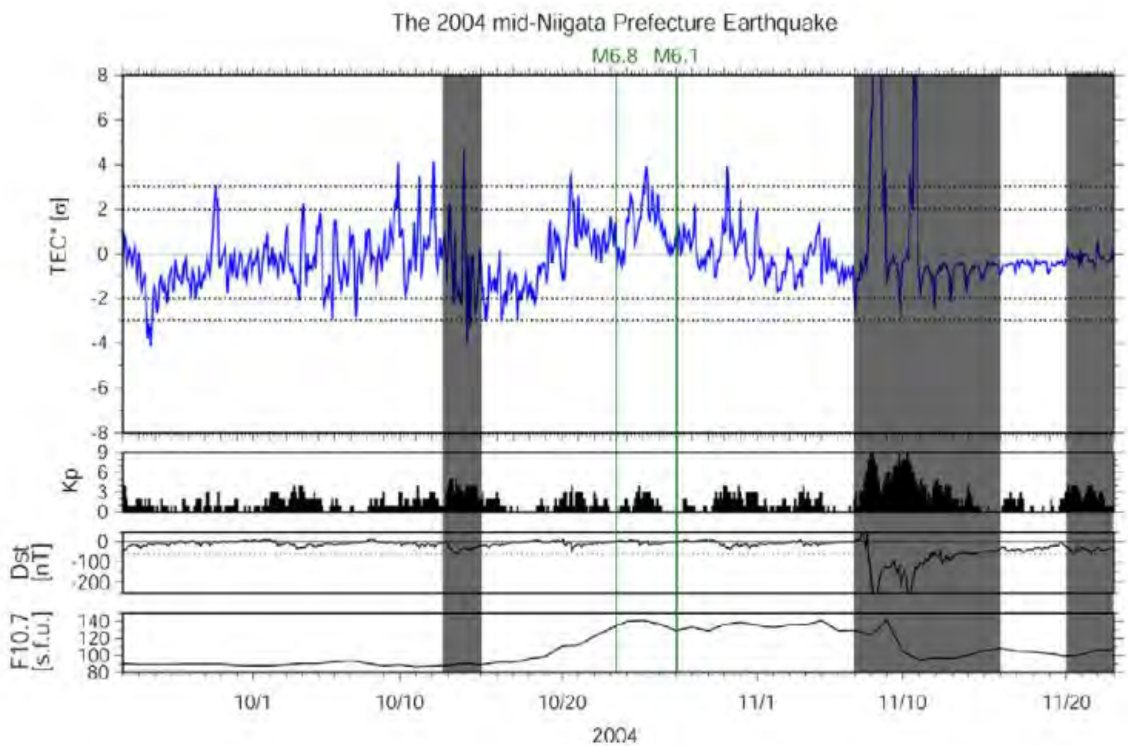

Sample of normalized GIM-TEC plot from Kon et. al.'s study on the mid-Niigata Perfecture Earthquake*

*S. Kon, M. Nishihashi, K. Hattori, Ionospheric anomalies possibly associated with M > 6.0 earthquakes in the Japan area during 1998-2010; Case studies and statistical study, Journal of Asian Earth Sciences, 41 (2011) 410-420

Ionospheric Perturbations – GPS-TEC

Quartile-Based Method

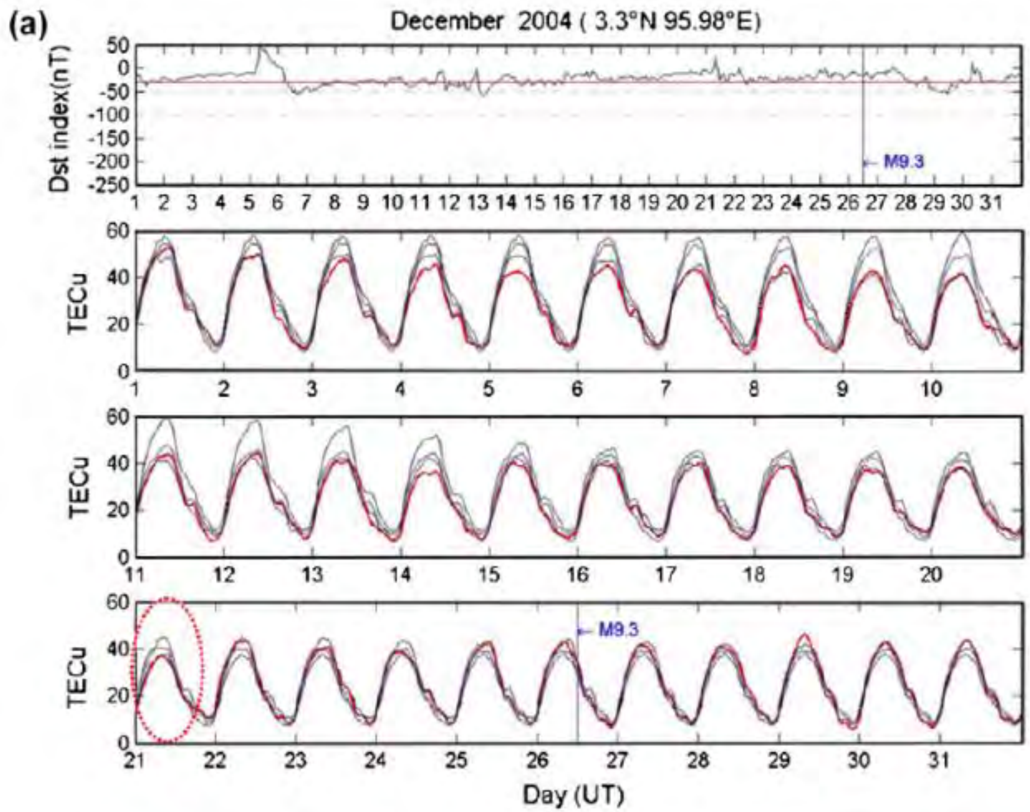

- Median of previous 15-days
- First quartile
- Third quartile

Sample of quartile-based method plot from Liu et. al.'s study M9.5 Sumatra earthquake*

*Liu, C.Y., Liu, J.Y., Chen, W.S., Li, J.Z., Xia, Y.Q., Cui, X.Y., An integrated study of anomalies observed before four major earthquakes: 2004 Sumatra M9.3, 2006 Pingtung M7.0, 2007 Cheetsu Oki M6.8 and 2008 Wenchuan M8.0, Journal of Asian Earth Sciences 41 (2011) 401-409

- Normalized GIM-TEC – M6.9 Negros Oriental Earthquake

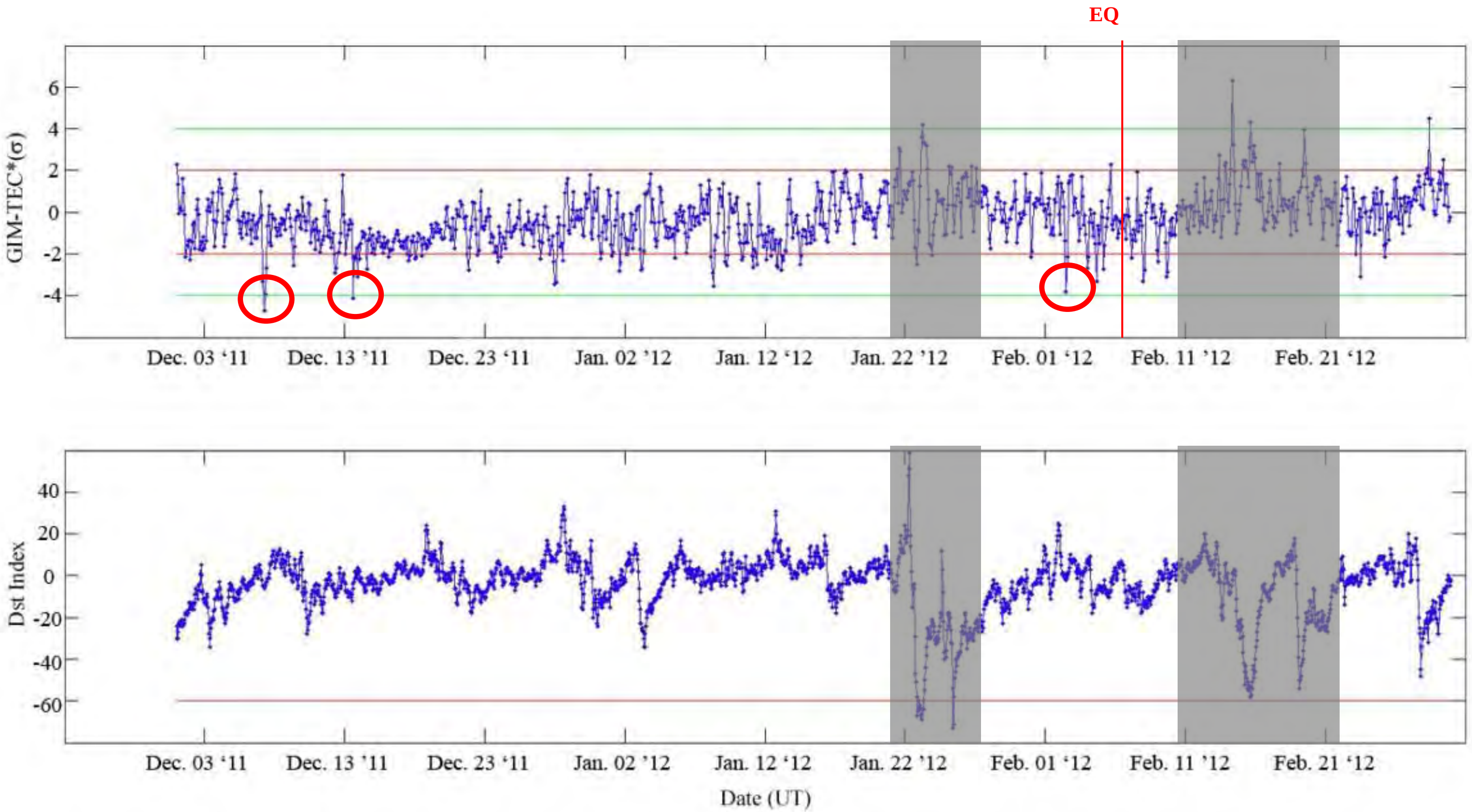

Normalized GIM-TEC(σ) as well as Dst index as a function of Date in UT for the M6.9 Negros Oriental Earthquake on Feb. 6, 2012

- Normalized GIM-TEC – M7.6 Eastern Samar Earthquake

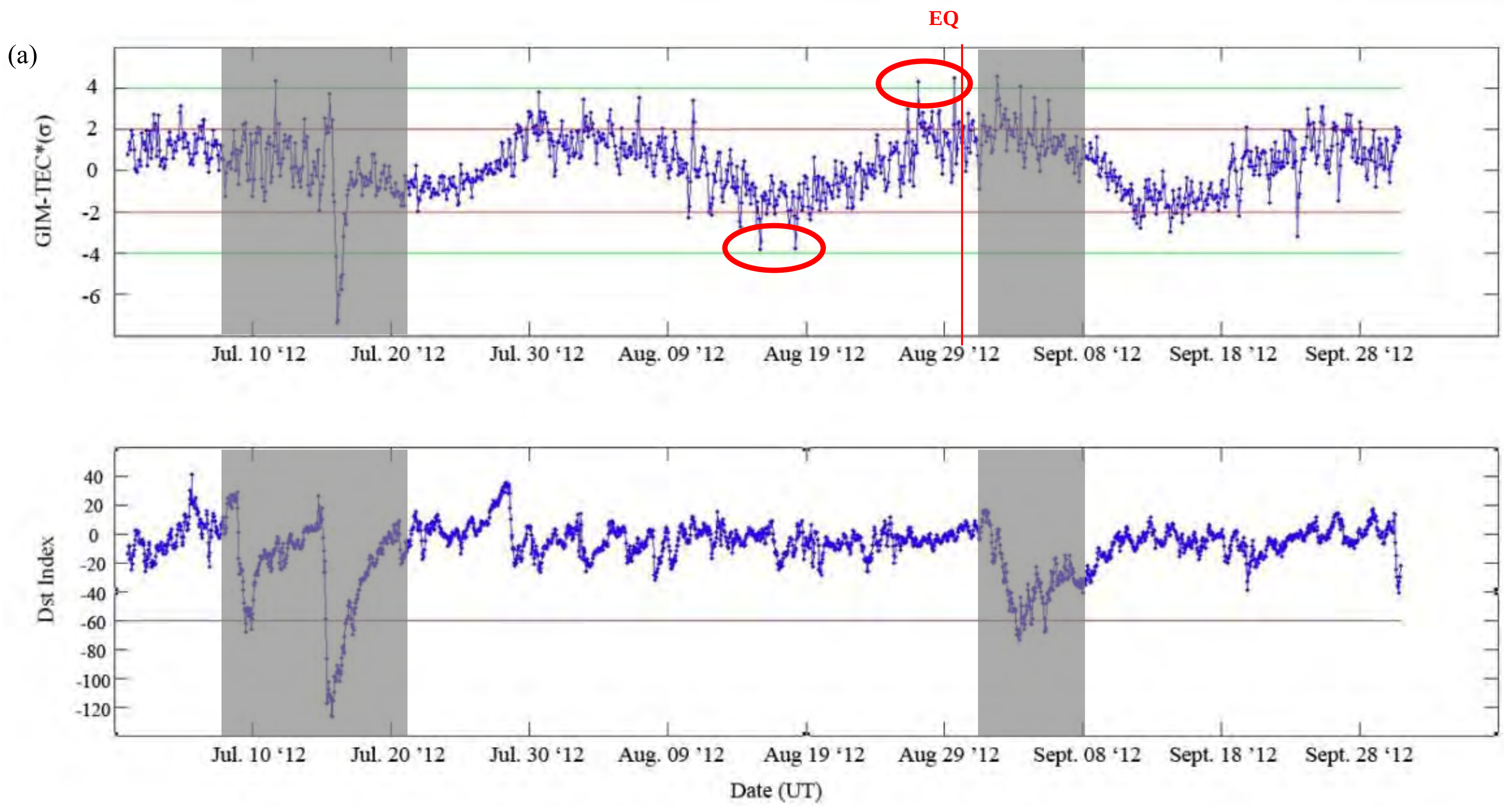

Normalized GIM-TEC(σ) as well as Dst index as a function of Date in UT for the M7.6 Eastern Samar Earthquake on August 31, 2012

- Normalized GIM-TEC – M7.2 Bohol Earthquake

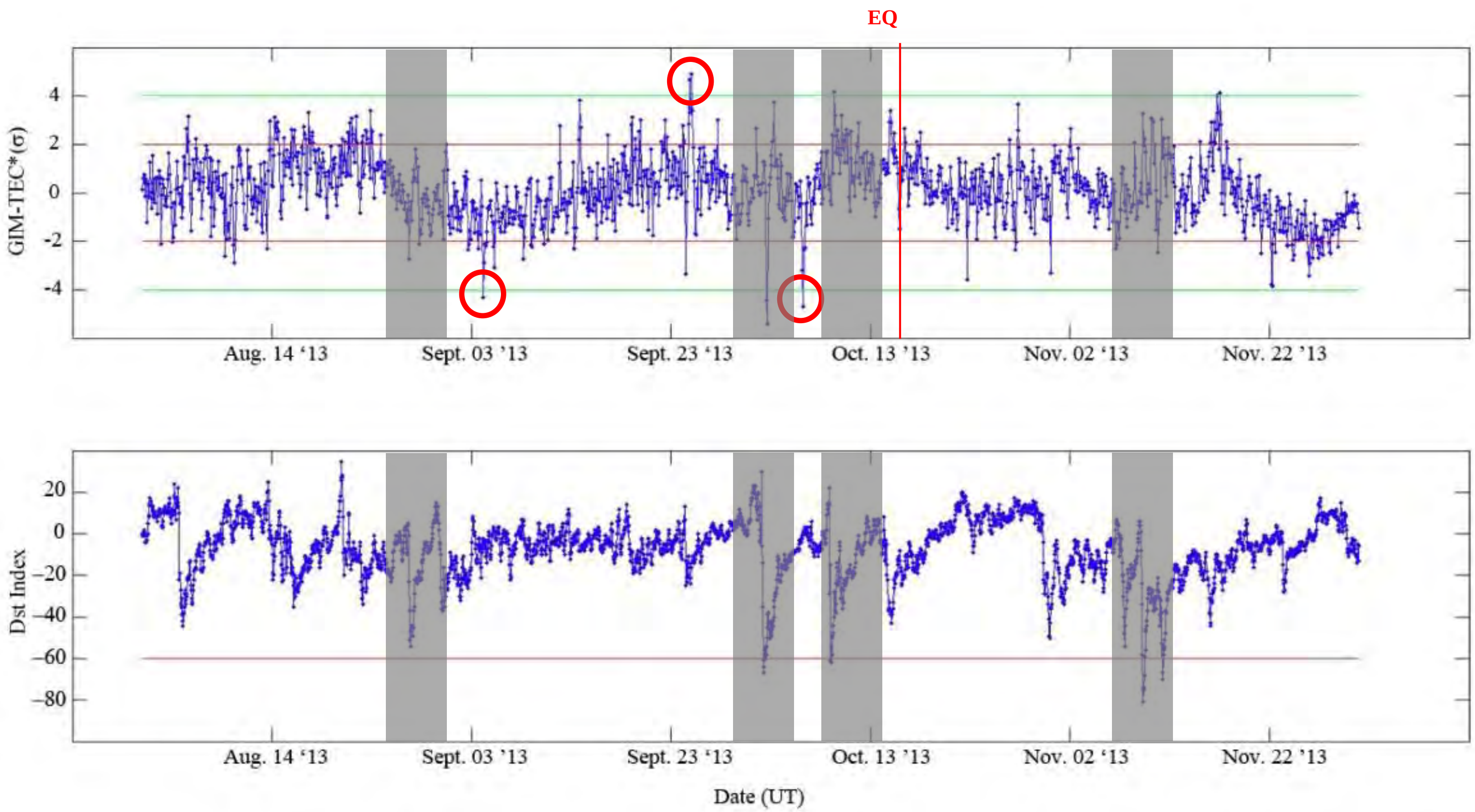

Normalized GIM-TEC(σ) as well as Dst index as a function of Date in UT for the M7.2 Bohol Earthquake on October 15, 2013

- Quartile-Based Method– M6.9 Negros Oriental Earthquake

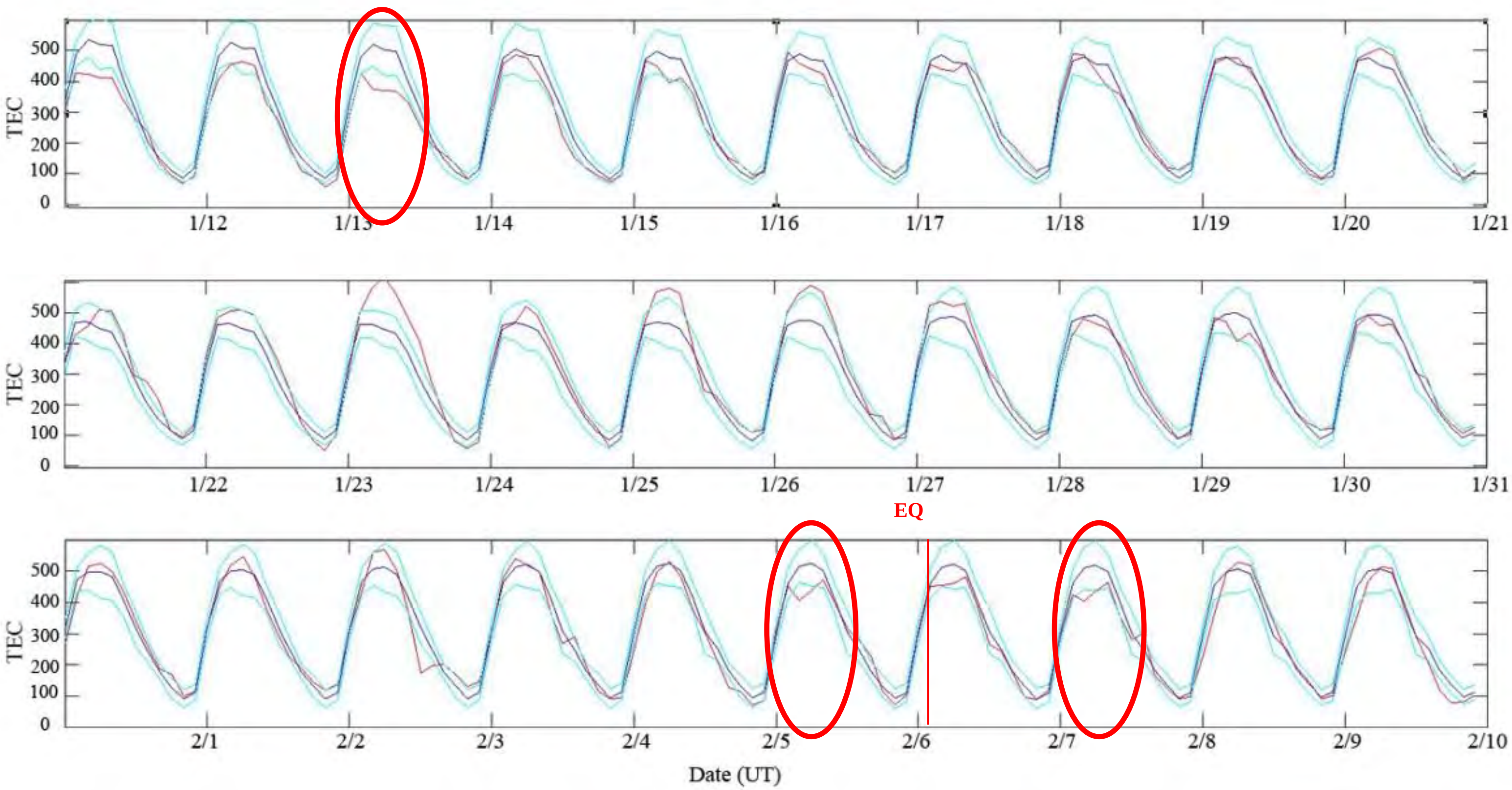

Quartile – Based TEC as a function of Date in UT for M6.9 Negros Oriental Earthquake

15-day mean, Upper and Lower Quartiles, Actual Data

- Quartile-Based Method– M7.6 Eastern Samar Earthquake

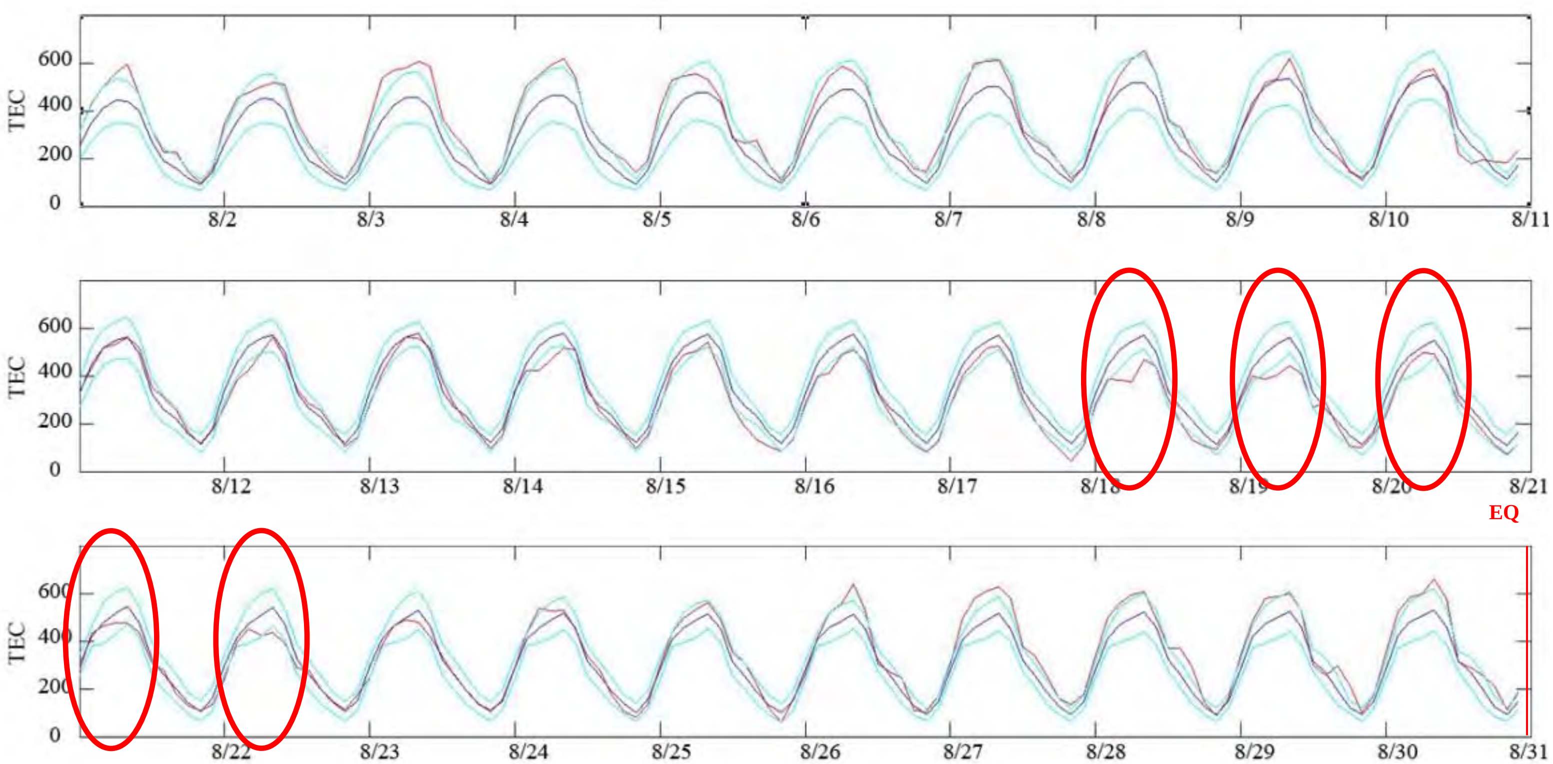

Quartile – Based TEC as a function of Date in UT for M7.6 Eastern Samar Earthquake

15-day mean, Upper and Lower Quartiles, Actual Data

- Quartile-Based Method– M7.2 Bohol Earthquake

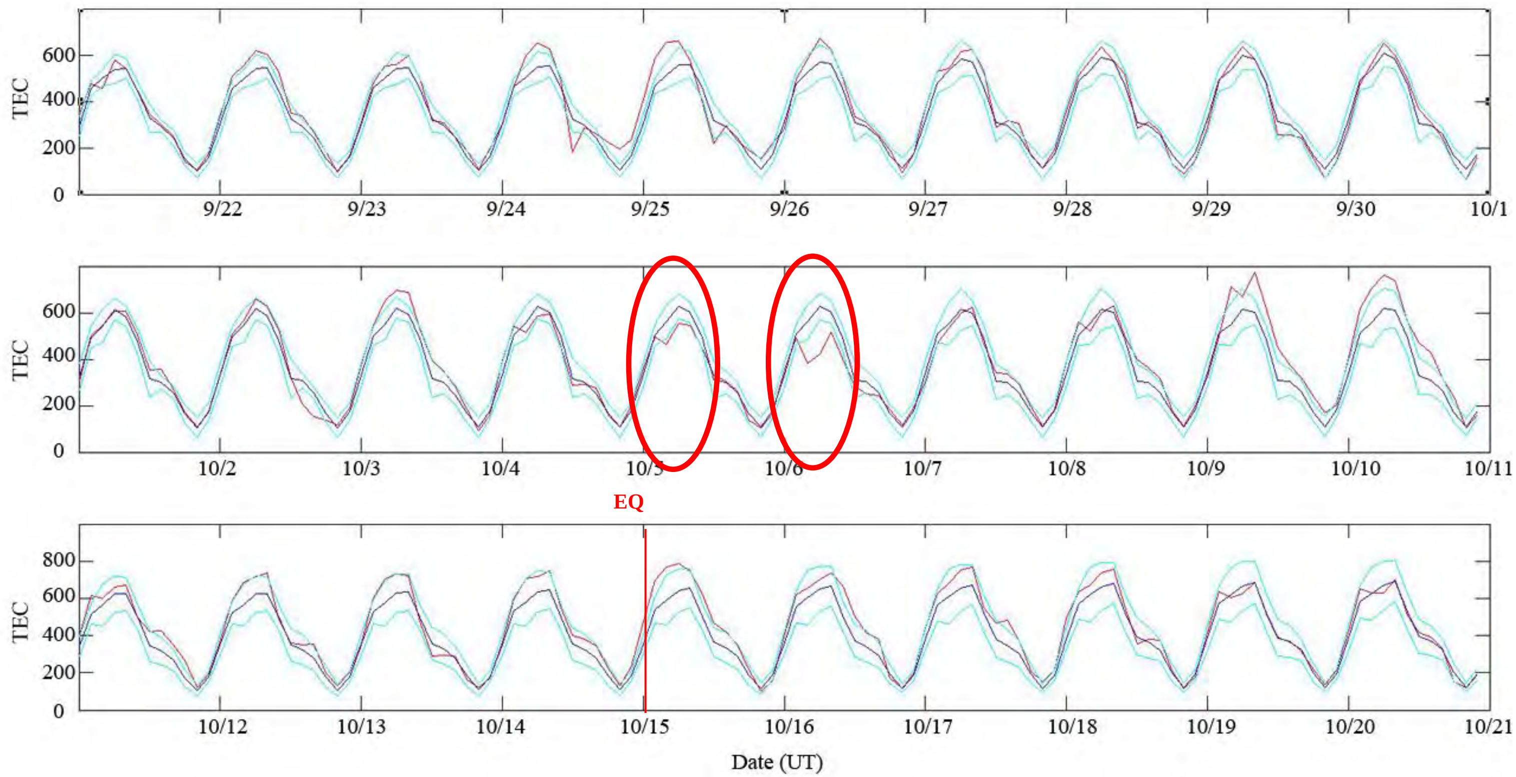

Quartile-Based TEC as a function of Date in UT for the M7.2 Bohol Earthquake

15-day mean, Upper and Lower Quartiles, Actual Data

Moro Gulf Earthquake – October 4, 2009

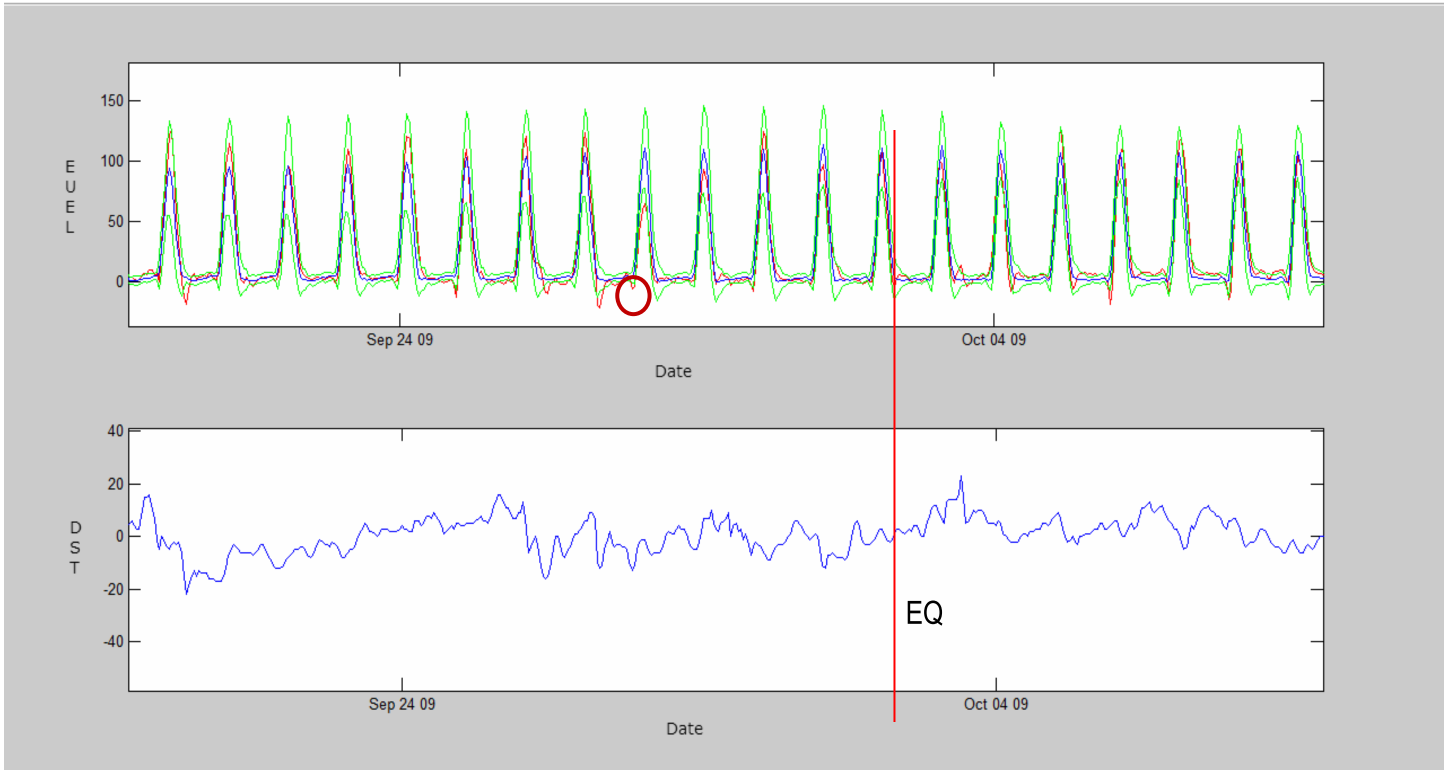

Davao EEJ against normal Davao EEJ

M6.9 Negros Earthquake– February 6, 2012

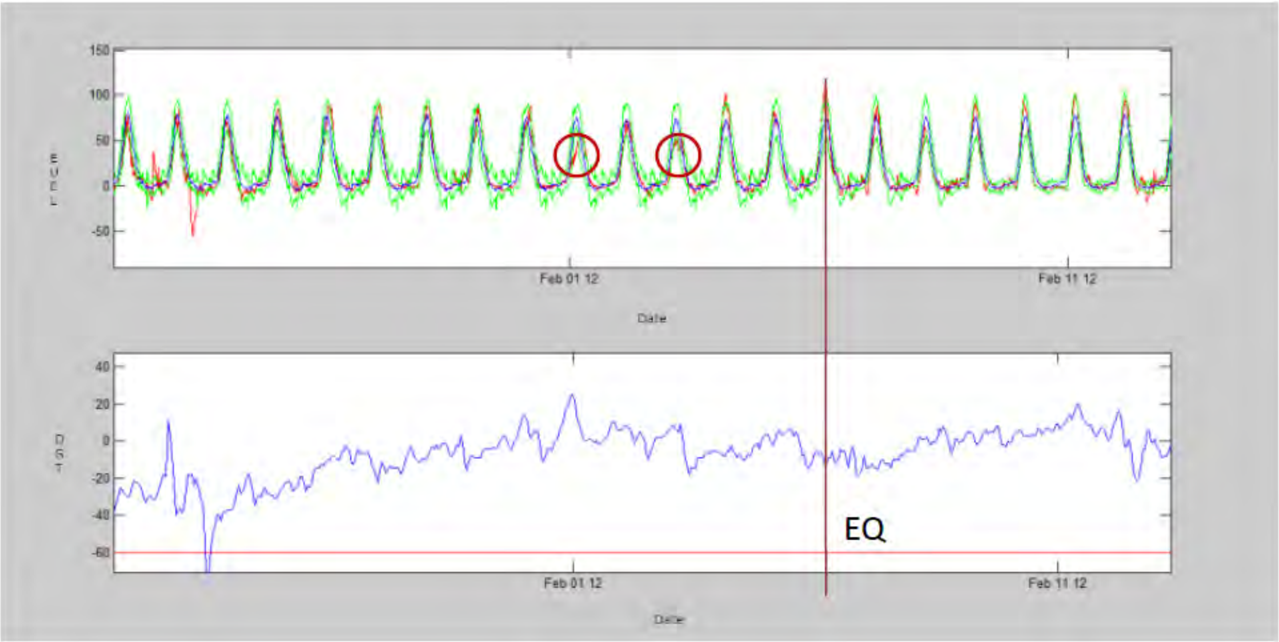

Cebu EEJ data

Change in Height of the Ionosphere

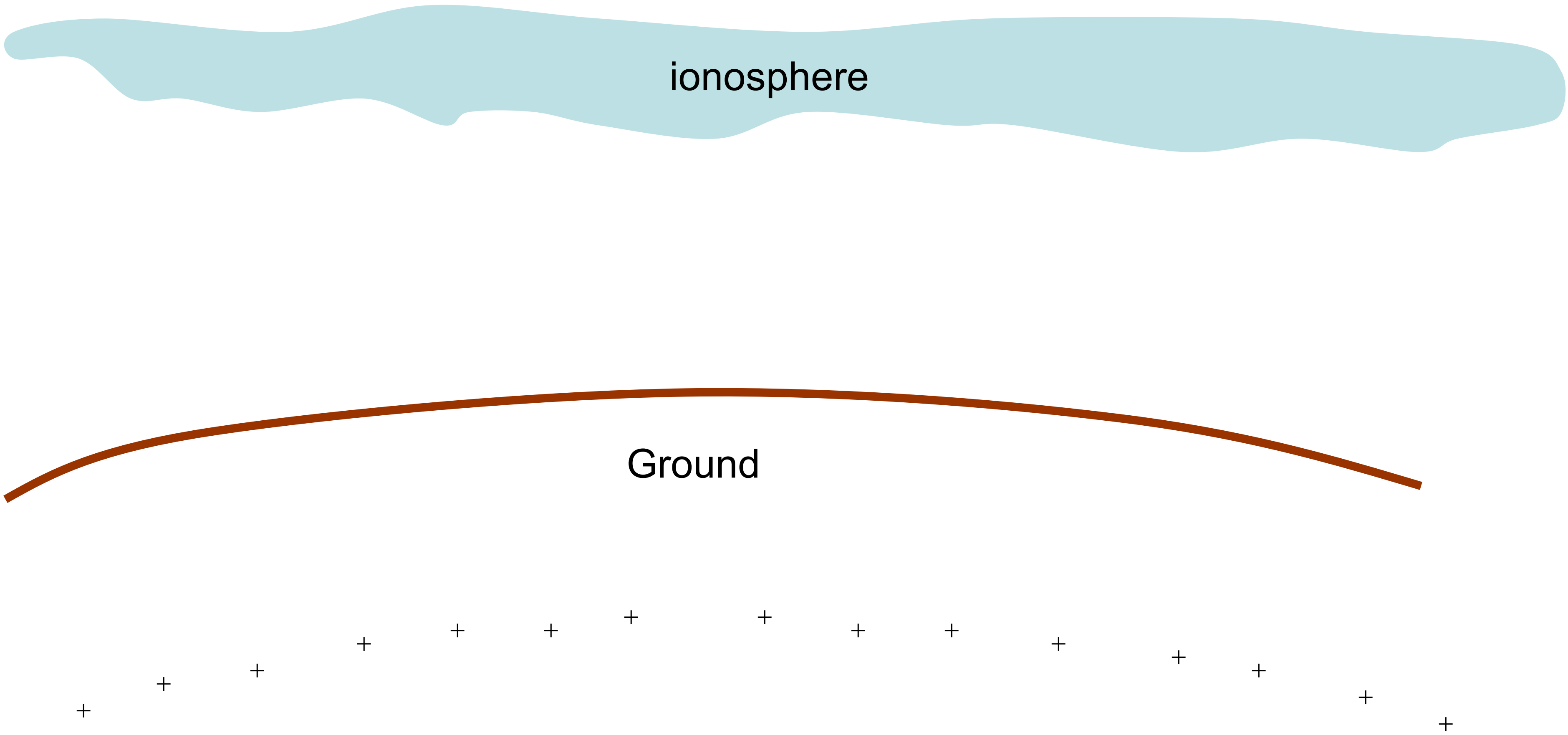

Summary:

1. A new index was developed to study EEJ using MAGDAS/CPMN data
2. A new ULF method was also developed for seismoelectromagnetic studies using MAGDAS/CPMN data
3. Electromagnetic precursors were detected in some earthquakes using the above method
4. We have demonstrated the possibility of using GPS-TEC for seismoelectromagnetics
5. EEJ magnitude anomaly using MAGDAS/CPMN data due to earthquake is possible

Thank You